October 21, 1974

To the Graduate Council:

I am submitting herewith a thesis written by James L. Taylor entitled "A Technique for Mapping Aircraft Stability Boundaries with Simultaneous Variations in Dynamic Stability Derivatives." I recommend that it be accepted in partial fulfillment of the requirements for the degree of Master of Science, with a major in Mathematics.

Kenneth R. Kimble

Kenneth R. Kimble, Major Professor

We have read this thesis
and recommend its acceptance:

T C Reddy

N. L. Loeffler

Accepted for the Council:

Hilton A. Smith

Vice Chancellor
Graduate Studies and Research

A TECHNIQUE FOR MAPPING AIRCRAFT STABILITY BOUNDARIES WITH SIMULTANEOUS VARIATIONS IN DYNAMIC STABILITY DERIVATIVES

A Thesis

Presented for the

Master of Science

Degree

The University of Tennessee

James L. Taylor

December 1974

ACKNOWLEDGMENTS

The author wishes to express his appreciation to the officials of the Air Force and ARO, Inc., for the opportunity to attend The University of Tennessee Space Institute. The author is particularly indebted to: Mr. M. D. Johnson, Propulsion Wind Tunnel (PWT) Instrument Branch Manager; Mr. M. L. McKee, 16 Foot Test Instrumentation Section Supervisor; Mr. J. R. Lancaster, PWT Instrument Branch Staff Engineer; and Mr. R. W. Butler, 4T Projects Branch Development Section Engineer, for their valuable suggestions and advice during the development of this study. The author wishes to express his appreciation to his advisor, Dr. K. R. Kimble, Professor of Mathematics, The University of Tennessee Space Institute, for his valuable assistance and advice.

The research reported herein was sponsored by Headquarters, Arnold Engineering Development Center, Arnold Air Force Station, Tennessee, within the terms of Contract F40600-75-C-0001 with ARO, Inc. Further reproduction is authorized to satisfy the needs of the United States Government.

1176531

ABSTRACT

This study presents a method for determining the effect that variations in design parameters may have upon the transient response characteristics of a system of differential equations. The effects of single design parameter variations are described using a modified root locus technique. Simultaneous variations of two or three parameters are described using stability region maps.

The method employed for investigating system stability utilizes a linear approximation to determine how parameter variations affect the roots of the related characteristic equation. The approximation used is based on a Taylor series expansion of the system's characteristic equation.

A computer program has been written which applies the approximating technique to determining how simultaneous variations in aerodynamic parameters affect the transient response characteristics of an aircraft. Some sample results obtained using the computer program are included to illustrate the application.

TABLE OF CONTENTS

CHAPTER		PAGE
I.	INTRODUCTION	1
II.	FORMULATIONS	4
III.	MODIFIED ROOT LOCUS	10
	Example III-1	15
IV.	STABILITY REGION MAPPING	24
	Introduction	24
	Region Boundary	26
	Example IV-1	29
	Region Characteristics	37
	Three-dimensional Regions	41
V.	EFFECTS OF PARAMETER VARIATIONS ON AIRCRAFT LATERAL STABILITY	42
	Introduction	42
	Program Description	43
	Root locus	46
	Stability region mapping	50
	Program Outputs	59
BIBLIOGRAPHY		70
APPENDICES		72
VITA		81

LIST OF FIGURES

FIGURE		PAGE
1.	Root Locus Showing the Effects of Increasing Design Parameter x_1 from the Base Value	19
2.	Root Locus Showing the Effects of Decreasing Design Parameter x_1 from the Base Value	21
3.	Stability Region Map for Example IV-1	33
4.	Detailed Stability Region Map for Example IV-1. .	39
5.	Basic Flow Chart for Lateral Stability Investigation Computer Program.	44
6.	Flow Diagram of Root Locus Subroutine	47
7.	Tangent Vector Possibilities.	52
8.	Dual Direction Possibilities, Opposite Slope Signs.	54
9.	Dual Direction Possibilities, Same Slope Signs.	55
10.	Corner Point Tangent Vector Possibilities	56
11.	Arbitrary Stability Region Map.	58
12.	Flow Diagram of Boundary Mapping Routine.	60
13.	Sample Root Locus Plot Obtained Using the Lateral Stability Computer Program.	64
14.	Sample Stability Region Map Obtained Using the Lateral Stability Computer Program.	66

FIGURE PAGE

15. Detailed Stability Map Illustrating the Spiral and Roll Roots 68

16. Detailed Stability Map Illustrating the Dutch Roll Roots. 69

CHAPTER I

INTRODUCTION

In analyzing a physical system which is governed by a system of differential equations, it is desirable to determine the effects that variations in related system design parameters have upon the system's transient response. If the governing differential equations are linear with constant coefficients, then an investigation of the effects of parameter variations can be accomplished by examining the behavior of the roots of the associated characteristic equation. Requiring that the roots have negative real parts is both necessary and sufficient for stability [1].[1]

For example, consider a physical system described by the following equation:

$$m\ddot{x} + 2h\dot{x} + k^2x = 0 \qquad \text{(I-1)}$$

where m, h, and k are non-zero design parameters. By letting

$$x_1 = x \ , \qquad \text{(I-2)}$$

$$x_2 = \dot{x}_1 = \dot{x} \ , \qquad \text{(I-3)}$$

---

[1] Numbers in brackets refer to similarly numbered references in the bibliography.

Equation (I-1) may be rewritten as:

$$\dot{x}_1 = x_2 \ , \tag{I-4}$$

$$\dot{x}_2 = \ddot{x} = - k^2/m \ x_1 - 2h/m \ x_2 \ , \tag{I-5}$$

which can be expressed as:

$$\begin{bmatrix} 0 & 1 \\ \frac{-k^2}{m} & \frac{-2h}{m} \end{bmatrix} \begin{bmatrix} x_1 \\ x_2 \end{bmatrix} = \begin{bmatrix} \dot{x}_1 \\ \dot{x}_2 \end{bmatrix} . \tag{I-6}$$

This can be expressed in matrix notation as:

$$A\vec{X} = \dot{\vec{X}} \ . \tag{I-7}$$

By assuming a solution of the form

$$\vec{X} = e^{\lambda t}\vec{Y} \ , \tag{I-8}$$

Equation (I-7) becomes

$$(A-\lambda I)\vec{Y} = 0 \ , \tag{I-9}$$

where I is the identity matrix. Equation (I-9) represents a system of linear homogeneous equations and has a non-trivial solution if the determinant of $(A-\lambda I)$ is zero. The determinant of $(A-\lambda I)$ is referred to as the characteristic equation and is given by:

$$\det(A-\lambda I) = \lambda^2 + 2h/m \ \lambda + k^2/m = 0 \ . \tag{I-10}$$

If the roots of Equation (I-10) have negative real parts, then the system described by Equation (I-1) is said to be stable. Hence the solution to the homogeneous differential equation can be determined by finding the eigenvalues of the matrix A. If the eigenvalues have negative real parts, then the solution is said to be stable.

The coefficients of the characteristic equation are functions of the design parameters, m, h, and k. The effects of variations in these parameters can be investigated by examining the behavior of the roots of the characteristic equation. This process is generally referred to as a parametric study.

The method presented in the following material was developed to investigate the effects that variations in aerodynamic parameters have upon the transient response characteristics of an aircraft. The method, which is based upon the movement of the roots of the characteristic equation, is presented in generalized form and is illustrated with simple examples. An example of the technique applied to investigating aircraft lateral stability is also presented. For variations in one design parameter, the effects on stability are represented using root locus. For simultaneous parameter variations, the effects on stability are represented using stability region maps.

CHAPTER II

FORMULATIONS

Consider the following characteristic equation of degree, n:

$$G \equiv \sum_{i=0}^{n} F_i(\vec{X})\lambda^i = 0 \ , \qquad \text{(II-1)}$$

where

$$\vec{X} = (x_1, x_2, \cdots, x_\ell) \qquad \text{(II-2)}$$

are defined as design parameters, and $F_i(\vec{X})$ are real valued functions which have continuous first partial derivatives with respect to $\vec{X}$. Note that λ is a function of $\vec{X}$,

$$\{\lambda_k(\vec{X})\} \equiv \vec{\lambda}(\vec{X}) \ , \qquad \text{(II-3)}$$

and is chosen such that G is identically zero. By taking the total differential of G, the following equation is obtained:

$$dG = \left(\frac{\partial G}{\partial \lambda}\right)_{\vec{P}_k^m} d\lambda_k + \left(\frac{\partial G}{\partial x_1}\right)_{\vec{P}_k^m} dx_1 + \cdots + \left(\frac{\partial G}{\partial x_\ell}\right)_{\vec{P}_k^m} dx_\ell = 0 \ , \qquad \text{(II-4)}$$

where

$$\frac{\partial G}{\partial x_j} = \sum_{i=0}^{n} \frac{\partial F_i}{\partial x_j}(\lambda^i) \quad , \quad 1 \leq j \leq \ell \quad , \tag{II-5}$$

and

$$\frac{\partial G}{\partial \lambda} = \sum_{i=1}^{n} i\lambda^{i-1} F_i(\vec{X}) \quad . \tag{II-6}$$

As indicated, the partial derivatives in Equation (II-4) are to be evaluated at a point, $\vec{P}_k^m$, where

$$\vec{P}_k^m = (x_1^m, x_2^m, \cdots, x_\ell^m, \lambda_k) \quad . \tag{II-7}$$

For a characteristic equation of degree, n, the expression for dG represents a system of n homogeneous linear equations. By rewriting Equation (II-4) the following system of equations is obtained:

$$d\lambda_1 = -\left(\frac{1}{\frac{\partial G}{\partial \lambda}}\right)_{\vec{P}_1^m} \left\{ \left(\frac{\partial G}{\partial x_1}\right)_{\vec{P}_1^m} dx_1 + \cdots + \left(\frac{\partial G}{\partial x_\ell}\right)_{\vec{P}_1^m} dx_\ell \right\} ,$$

$$d\lambda_2 = -\left(\frac{1}{\frac{\partial G}{\partial \lambda}}\right)_{\vec{P}_2^m} \left\{ \left(\frac{\partial G}{\partial x_1}\right)_{\vec{P}_2^m} dx_1 + \cdots + \left(\frac{\partial G}{\partial x_\ell}\right)_{\vec{P}_2^m} dx_\ell \right\} ,$$

$$\vdots$$

$$d\lambda_n = -\left(\frac{1}{\frac{\partial G}{\partial \lambda}}\right)_{\vec{P}_n^m} \left\{ \left(\frac{\partial G}{\partial x_1}\right)_{\vec{P}_n^m} dx_1 + \cdots + \left(\frac{\partial G}{\partial x_\ell}\right)_{\vec{P}_n^m} dx_\ell \right\} , \tag{II-8}$$

which can be put in the matrix form:

$$d\vec{\lambda} = A d\vec{X} \ , \qquad \text{(II-9)}$$

where $d\vec{\lambda}$ is a column vector of n components, $d\vec{X}$ is a column vector of m components, and A is an n x ℓ matrix whose elements are complex. In general,

$$A_{i,j} = - \left(\frac{\partial G}{\partial x_j}\right)_{\vec{P}_i^k} \Big/ \left(\frac{\partial G}{\partial \lambda}\right)_{\vec{P}_i^k} \ , \qquad \text{(II-10)}$$

and is complex whenever λ_i is complex.

The system of linear equations described by Equation (II-8) gives a linear approximation for changes in each root. It is valid unless

$$\left(\frac{\partial G}{\partial \lambda}\right)_{\vec{P}_i^k} \ ,$$

which appears in the denominator of the $A_{i,j}$ element, vanishes. It may be shown that

$$\left(\frac{\partial G}{\partial \lambda}\right)_{\vec{P}_i^k}$$

vanishes only when λ_i occurs as a multiple root of G.

An equivalent way of obtaining the linear approximation is to expand the function, G, in a Taylor series about the point, $\vec{P}^0$ [2]. The first variation of G gives a linear approximation to the changes in the roots as a

function of changes in the design parameters. The resulting linear system is again given by Equation (II-9).

By approximating $d\vec{\lambda}$ by $\Delta\vec{\lambda}$ and $d\vec{X}$ by $\Delta\vec{X}$, Equation (II-9) becomes:

$$\Delta\vec{\lambda} = A\Delta\vec{X} \ . \qquad \text{(II-11)}$$

By specifying $\Delta\vec{X}$, the corresponding changes in $\Delta\vec{\lambda}$ may be determined. Equation (II-11) represents a system of linear equations which relate changes in each root as a function of changes in the design parameters. By specifying only small changes in $\vec{X}$, the error in the approximation should be small. This seems to indicate that one must be very conservative in determining $\Delta\vec{X}$ and must re-solve the characteristic equation to determine the error in the roots. If this were true, then little could be gained from the approximation and one could simply re-solve the characteristic equation repeatedly to determine the effects of variations in the design parameters. Fortunately, there are several readily available estimates of error which eliminate the necessity for re-solving the characteristic equation to determine the error in the approximation.

The characteristic equation, G, is an algebraic equation with real coefficients. As such, there are definite relationships between the coefficients and the roots. For a characteristic equation of the form given by Equation (II-1), the product of the roots is given by:

$$(-1)^n (\lambda_1 \lambda_2 \cdots \lambda_n) = F_o(\vec{X})/F_n(\vec{X}) \ , \qquad \text{(II-12)}$$

and the sum of the roots is given by

$$-(\lambda_1 + \lambda_2 + \cdots + \lambda_n) = F_{n-1}(\vec{X})/F_n(\vec{X}) \ . \qquad \text{(II-13)}$$

Similarly, other relationships exist between the roots and remaining coefficients of G [3]. Either Equation (II-12) or Equation (II-13) can be used to determine the error in the roots introduced by using the approximation. This eliminates the necessity of solving the characteristic equation to estimate the error and provides a means whereby the approximating technique given by Equation (II-11) can be optimized. The error estimate and the optimization are discussed later in conjunction with the root locus and boundary mapping applications.

The basis of the root movement technique is the system of linear approximating equations given by Equation (II-11). The effects that variations in the design parameters have on each root of the characteristic equation are given as a weighted sum of the incremental changes in the design parameters, where the weights are given by Equation (II-10). The relative weights assigned each incremental design parameter may be used to rank the design parameters according to relative importance for each root at

a particular point. For systems containing a large number of design parameters, the ability to select only the most significant parameters for investigation is extremely useful.

CHAPTER III

MODIFIED ROOT LOCUS

As an application of the root movement technique, consider the problem of determining the effect that variations in one design parameter has upon a system's transient response characteristics. The effects of perturbations in one design parameter may be completely described by examining the movement of the roots of the characteristic equation. As the design parameter takes on values ranging from plus infinity to minus infinity, the roots of the characteristic equation move in the complex plane along trajectories such that the characteristic equation remains identically zero. A complex plane plot of the trajectories of the roots is referred to as a root locus plot. By examining the root locus, the effects that changes in a particular design parameter have upon both the frequency and damping of each root may be described.

The process of a one-dimensional parameter investigation is described as a modified root locus technique to indicate that the root movement approximation described in Chapter II is used to generate the loci.

To initiate the process, select nominal values for all design parameters and solve the characteristic equation to determine the corresponding roots. That is, choose $\vec{X}^0$

and find $\vec{\lambda}(\vec{X})$. The initial starting point is referred to as the base point and the corresponding roots of the characteristic equation are referred to as the poles. The loci emanate from the poles and terminate at either infinity or at points in the complex plane referred to as zeroes. The zero points are defined to be points in the complex plane where the roots of the characteristic equation cluster about as the parameter being investigated takes on values near infinity. For a characteristic equation of the form, G, given by Equation (II-1), the cluster points or zeroes are determined as the roots of the following equation:

$$H \equiv \sum_{i=0}^{n} \left(\frac{\partial F_i(\vec{X})}{\partial x_j}\right)_{\vec{P}^0} \lambda^i = 0 \ , \qquad \text{(III-1)}$$

where x_j is the design parameter, and the partial derivatives are to be evaluated at the base point.

Starting at the base point, the incremental changes in each root are calculated using Equation (II-11), where the vector, $\Delta\vec{X}$, contains one non-zero entry corresponding to the design parameter being investigated. For example, if the x_j design parameter is to be investigated, then $\Delta\vec{X}$ has zero entries everywhere except in the jth position. The jth position of $\Delta\vec{X}$ contains an entry corresponding to the incremental change to be given to x_j. The incremental change is referred to as the step size. As noted previously, A is an n x ℓ matrix with complex elements

of the form given by Equation (II-10), where the partial derivatives are to be evaluated at the kth point, $\vec{P}_i^k$, where

$$\vec{P}_i^k = (x_1^k, x_2^k, \cdots, x_\ell^k, \lambda_i) \ . \qquad \text{(III-2)}$$

Notice that for an investigation of the x_j parameter,

$$\vec{P}_i^k = (x_1^0, x_2^0, \cdots, x_j^k, \cdots, x_\ell^0, \lambda_i) \ , \qquad \text{(III-3)}$$

where the superscript, 0, is used to indicate the base point values of the other m-1 parameters. Using the incremental changes found above for the roots, define the roots at the k+1 point as:

$$\vec{\lambda}^{k+1} = \vec{\lambda}^k + \Delta\vec{\lambda}^{k+1} \ . \qquad \text{(III-4)}$$

In addition, the vector, $\vec{X}$, at the k+1 point is defined as:

$$\vec{X}^{k+1} = \vec{X}^k + \Delta\vec{X}^{k+1} \ . \qquad \text{(III-5)}$$

Having found $\vec{\lambda}^{k+1}$ by using the approximation, the error in the roots may be estimated as follows. The relationships between the coefficients of G and the roots were previously mentioned in Chapter II. If G is an nth degree polynomial of the form given by Equation (II-1), then an estimate of the absolute error in the product of the roots at the kth point is defined as follows:

$$\text{error} = \left|\lambda_1^k \cdot \lambda_2^k \cdots \lambda_n^k\right| - \left|(-1)^n \frac{F_o(\vec{X}_k)}{F_n(\vec{X}_k)}\right| . \qquad \text{(III-6)}$$

Similarly, the error in the sum of the roots may be expressed as:

$$\text{error} = \left|\lambda_1+\lambda_2+\cdots+\lambda_n\right| - \left|\frac{F_{n-1}(\vec{X}_k)}{F_n(\vec{X}_k)}\right| . \qquad \text{(III-7)}$$

If the error at the kth point is small, the above process is repeated to find the k+1 point. However, if the error at the kth point is considered excessive, then G is re-solved to obtain a new starting point. The above process is then repeated.

It is reasonable to expect that a variable step size can be used in determining the movement of the roots. With the availability of an error estimate at each step, optimization of the technique can be accomplished as follows. If the error at the kth point is larger than a predetermined tolerance, then G is re-solved to establish a new starting point. If, in addition, the error determined at the k+1 point is also excessive, then the step size is halved and G is re-solved to define a new starting point. If, on the other hand, the error at both the kth and k+1 points is less than a predetermined tolerance, then the step size is doubled prior to finding the k+2 point. The commitment not to alter step size unless the same error

condition is encountered on two successive steps is intended to prevent racing; that is, constant doubling and halving.

The tolerance used in determining whether or not the error is excessive is determined empirically. If the tolerance used is liberal, then the trajectories of the roots will consist of linear segments which are piecewise continuous. Decreasing the permitted error tends to smooth the approximated trajectories. While the smoother trajectories are a more accurate representation of the loci, the increase in computer time may not be justifiable.

As stated earlier, the loci terminate at either the zeroes or at infinity. This provides a convenient way to terminate the process. It is only necessary to require that each zero point contain a root of G within some acceptable distance of it. For example, the process can terminate at the kth point only if each zero has a root of G near it.

As mentioned in Chapter II, the system of approximating equations is invalid at multiple root points because the denominator term of Equation (II-10) vanishes. In the complex plane the multiple root points are seen to be those points where the roots go from complex to real or vice-versa. At such points, the corresponding tangent vectors have infinite slope and hence, the characteristic equation will generally require re-solving at least once.

Example III-1

To illustrate some of the ideas discussed concerning the root locus technique, consider the following characteristic equation:

$$G = \lambda^2 + F_1(\vec{X})\lambda + F_0(\vec{X}) = 0 \ , \qquad \text{(III-8)}$$

where the coefficient functions are:

$$F_1(\vec{X}) = x_1 - x_2 \ , \qquad \text{(III-9)}$$

$$F_0(\vec{X}) = 0.25(x_1 + x_2) \ , \qquad \text{(III-10)}$$

where x_1 and x_2 represent design parameters. Assume that the base point, $\vec{P}^0$, is

$$\vec{P}^0 = (x_1^0, x_2^0) = (3,2) \ . \qquad \text{(III-11)}$$

At $\vec{P}^0$, the roots of G are

$$\lambda_1 = - 0.5 + j \ , \qquad \text{(III-12)}$$

$$\lambda_2 = - 0.5 - j \ , \qquad \text{(III-13)}$$

and are defined to be the poles, P_1 and P_2. The zero points corresponding to parameter x_1 are determined as the roots of the following equation:

$$H = \sum_{i=0}^{1} \left(\frac{\partial F_i(\vec{X})}{\partial x_j}\right)_{\vec{P}^0} \lambda^i = 0$$

$$= \left(\frac{\partial F_0(\vec{X})}{\partial x_1}\right)_{\vec{P}^0} + \left(\frac{\partial F_1(\vec{X})}{\partial x_1}\right)_{\vec{P}^0} \lambda$$

$$= 0.25 + \lambda \ . \qquad \text{(III-14)}$$

Hence, there is one zero point at $\lambda = -0.25$. The loci emanate from the poles, P_1 and P_2, and travel to the zero and to infinity. The trajectories for λ_1 and λ_2 may be determined using the linear approximation given by Equation (II-11). For this example, Equation (II-11) becomes:

$$\begin{bmatrix} \Delta\lambda_1 \\ \Delta\lambda_2 \end{bmatrix} = - \begin{bmatrix} (\partial G/\partial x_1 \,/\, \partial G/\partial\lambda)_{\vec{P}_1^0} & (\partial G/\partial x_2 \,/\, \partial G/\partial\lambda)_{\vec{P}_1^0} \\ (\partial G/\partial x_1 \,/\, \partial G/\partial\lambda)_{\vec{P}_2^0} & (\partial G/\partial x_2 \,/\, \partial G/\partial\lambda)_{\vec{P}_2^0} \end{bmatrix} \begin{bmatrix} \Delta x_1 \\ \Delta x_2 \end{bmatrix} \qquad \text{(III-15)}$$

where

$$\vec{P}_1^0 = (x_1^0, x_2^0, \lambda_1) \ , \qquad \text{(III-16)}$$

$$\vec{P}_2^0 = (x_1^0, x_2^0, \lambda_2) \ , \qquad \text{(III-17)}$$

$$\partial G/\partial x_1 = \lambda + 0.25 \ , \qquad \text{(III-18)}$$

$$\partial G/\partial x_2 = -\lambda + 0.25 \ , \qquad \text{(III-19)}$$

$$\partial G/\partial \lambda_1 = 2\,\lambda_1 + x_1 - x_2 \,, \qquad \text{(III-20)}$$

$$\partial G/\partial \lambda_2 = 2\,\lambda_2 + x_1 - x_2 \,. \qquad \text{(III-21)}$$

At the base point, $\vec{P}^0$, Equation (III-15) becomes:

$$\begin{bmatrix} \Delta\lambda_1 \\ \Delta\lambda_2 \end{bmatrix} = - \begin{bmatrix} (0.5+0.125j)\,(-0.5-0.375j) \\ (0.5-0.125j)\,(-0.5+0.375j) \end{bmatrix} \begin{bmatrix} \Delta x_1 \\ 0 \end{bmatrix}, \qquad \text{(III-22)}$$

Since Δx_2 is zero, Equation (III-22) simplifies to:

$$\Delta\lambda_1 = (-\,0.5 - 0.125j)\,\Delta x_1 \,, \qquad \text{(III-23)}$$

$$\Delta\lambda_2 = (-\,0.5 + 0.125j)\,\Delta x_1 \,. \qquad \text{(III-24)}$$

In the complex plane, Equations (III-23) and (III-24) represent vectors tangent to the eigenvalue trajectories at the poles, P_1 and P_2. By letting Δx_1 equal a step size of 0.1, an approximation to the roots at $\vec{P}^1$ can be obtained as follows:

$$\vec{\lambda}^1 = \vec{\lambda}^0 + \Delta\vec{\lambda}^0$$

$$\vec{\lambda}^1 = \begin{bmatrix} (-\,0.5 + j) \\ (-\,0.5 - j) \end{bmatrix} + \begin{bmatrix} (-0.05 - 0.012j) \\ (-\,0.05 + 0.012j) \end{bmatrix}$$

$$\vec{\lambda}^1 = \begin{bmatrix} (-\,0.55 + 0.99j) \\ (-\,0.55 - 0.99j) \end{bmatrix} \qquad \text{(III-25)}$$

The error estimate at $\vec{P}^1$ may be computed using Equation (III-6) as:

$$\text{error} = \left|\lambda_1^1 \ \lambda_2^1\right| - \frac{5.25}{4} = 0.01 \ . \qquad \text{(III-26)}$$

For a tolerance of 0.1, the root locus shown in Figure 1 was generated. Table I summarizes the computations.

The root locus drawing shown in Figure 1 illustrates the effects of increasing parameter, x_1, from its base value of 3.0. Using the approximation with step sizes of $\Delta x_1 = 0.1$ and 0.2, it was necessary only to re-compute the roots once. This occurred in the vicinity of the multiple root at $\lambda = -1.28$. In sketching the approximated trajectories for λ_1 and λ_2, the symbol, O, is used to represent the approximated λ value. The vector drawn from each symbol is the tangent vector computed at the λ value corresponding to that symbol.

By using a negative step size, the root locus showing the effects of decreasing parameter x_1 from its base value of 3.0 may be generated. Figure 2 shows both the approximated and actual trajectories for this case. In a similar manner, the root locus showing the effects of increasing and decreasing parameter x_2 may be generated. Table II summarizes the computation.

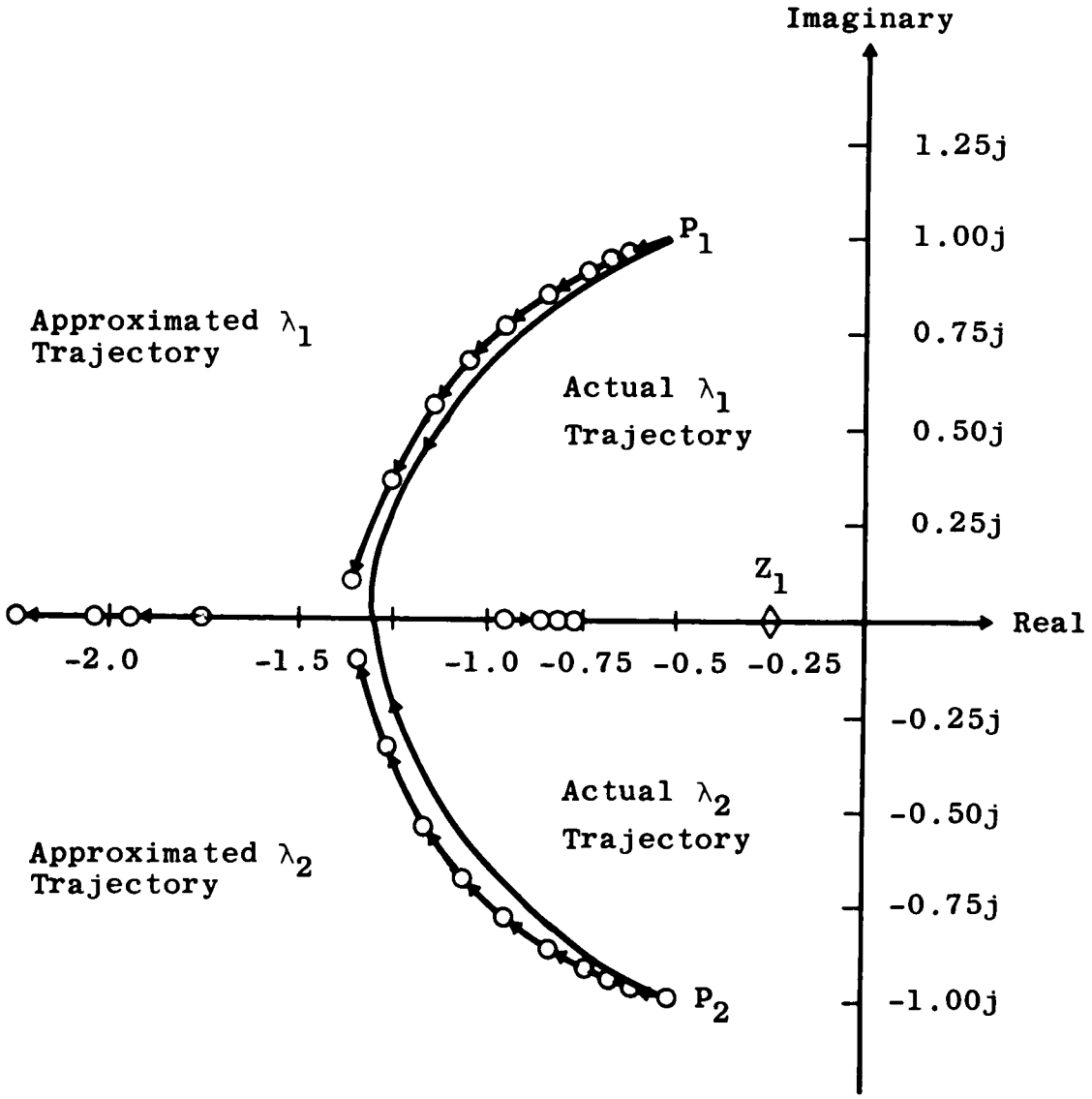


Figure 1. Root locus showing the effects of increasing design parameter x_1 from the base value.

TABLE I

SUMMARY OF COMPUTATIONS USED IN OBTAINING FIGURE 1

x_1	x_2	Tangent Vector(λ_1)	Tangent Vector(λ_2)	Approximate Roots	Actual Roots
3.0	2.0	-0.5 -0.125j	-0.5 +0.125j	-	-0.5 ± j
3.1	2.0	-0.5 -0.15 j	-0.5 +0.15 j	-0.55 ±0.99j	-0.55 ±0.95j
3.2	2.0	-0.5 -0.18 j	-0.5 +0.18 j	-0.6 ±0.97j	-0.6 ±0.95j
3.4	2.0	-0.5 -0.24 j	-0.5 +0.24 j	-0.7 ±0.93j	-0.7 ±0.9 j
3.7	2.0	-0.5 -0.35 j	-0.5 +0.35 j	-0.85 ±0.84j	-0.85 ±0.85j
4.1	2.0	-0.5 -0.6 j	-0.5 +0.6 j	-1.05 ±0.66j	-1.05 ±0.63j
4.5	2.0	-0.5 -1.4 j	-0.5 +1.4 j	-1.25 ±0.36j	-1.25 ±0.25j
4.7[a]	2.0	0.87+0 j	-1.87+0 j	-1.35 ±0.08j	-0.95,-1.75
4.8	2.0	0.56+0 j	-1.56+0 j	-0.86,-1.94	-0.9 ,-1.9
4.9	2.0	0.5 +0 j	-1.5 +0 j	-0.8 -2.1	-0.85,-2.05
5.0	2.0	0.33+0 j	-1.3 +0 j	-0.75,-2.25	-0.8 ,-2.2
5.2	2.0	-	-	-0.68,-2.51	-0.72,-2.48

[a]Re-started approximation at $x_1 = 4.7$.

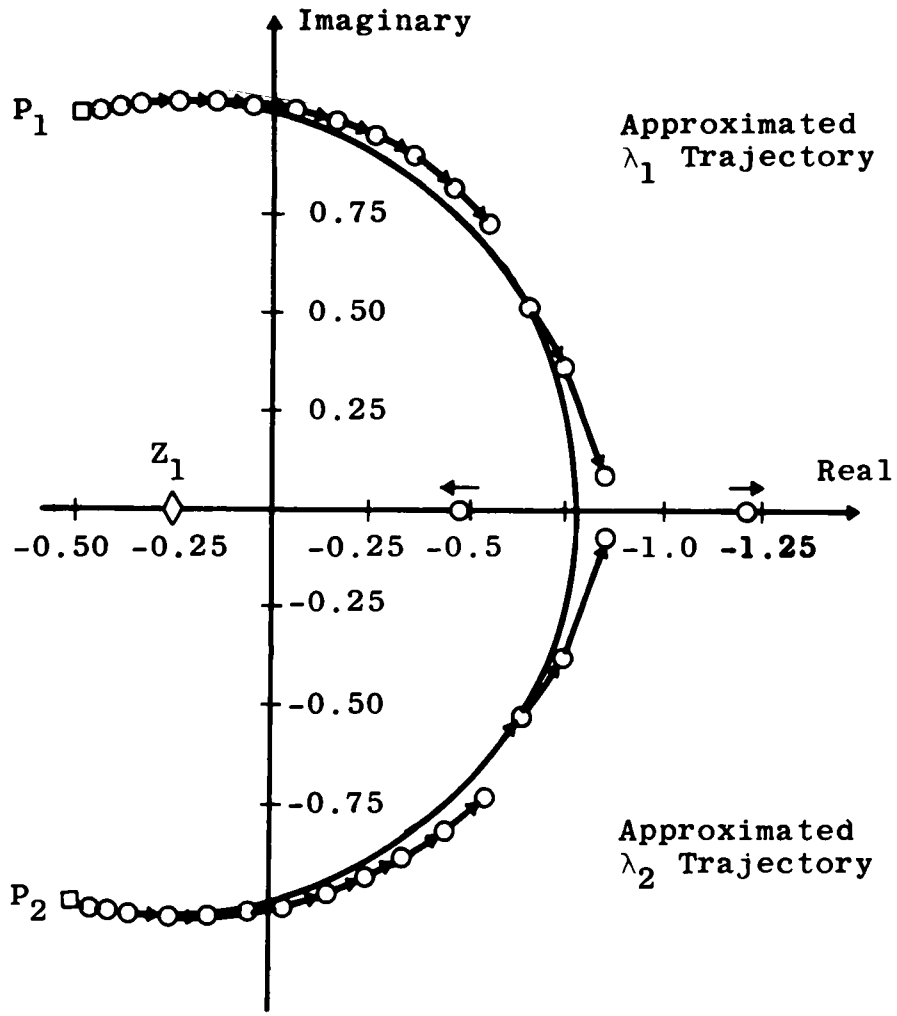


Figure 2. Root locus showing the effects of decreasing design parameter x_1 from the base value.

TABLE II

SUMMARY OF COMPUTATIONS USED IN OBTAINING FIGURE 2

x_1	x_2	Tangent Vector(λ_1)	Tangent Vector(λ_2)	Approximate Roots	Actual Roots
3.0	2.0	-0.5 +0.125j	-0.5 +0.125j	-	-0.50 $\pm$ j
2.9	2.0	-0.5 -0.1 j	-0.5 +0.1 j	-0.45 $\pm$1.01j	-0.45 $\pm$1.01j
2.8	2.0	-0.5 -0.075j	-0.5 +0.075j	-0.40 $\pm$1.02j	-0.40 $\pm$1.02j
2.7	2.0	-0.5 -0.05 j	-0.5 +0.05 j	-0.35 $\pm$1.03j	-0.35 $\pm$1.03j
2.5	2.0	-0.5 -0 j	-0.5 +0 j	-0.25 $\pm$1.04j	-0.25 $\pm$1.03j
2.3	2.0	-0.5 +0.05 j	-0.5 -0.05 j	-0.15 $\pm$1.04j	-0.15 $\pm$1.03j
2.1	2.0	-0.5 +0.10 j	-0.5 -0.10 j	-0.05 $\pm$1.03j	-0.05 $\pm$1.01j
1.7	2.0	-0.5 +0.2 j	-0.5 -0.2 j	+0.15 $\pm$0.98j	+0.15 $\pm$0.95j
1.5	2.0	-0.5 +0.253j	-0.5 -0.253j	+0.25 $\pm$0.94j	+0.25 $\pm$0.90j
1.3	2.0	-0.5 +0.34 j	-0.5 -0.34 j	+0.35 $\pm$0.89j	+0.35 $\pm$0.84j
1.1	2.0	-0.5 +0.43 j	-0.5 -0.43 j	+0.45 $\pm$0.82j	+0.45 $\pm$0.76j

TABLE II (continued)

x_1	x_2	Tangent Vector(λ_1)	Tangent Vector(λ_2)	Approximate Roots	Actual Roots
0.9[a]	2.0	-0.5 +0.62 j	-0.5 -0.62 j	+0.55 $\pm$0.73j	+0.55 $\pm$0.65j
0.5	2.0	-0.5 +1.4 j	-0.5 -1.4 j	+0.75 $\pm$0.36j	+0.75 $\pm$0.25j
0.3[a]	2.0	+0.95+0 j	-1.95+0 j	+0.85 $\pm$0.8 j	+0.47, 1.23
0.2	2.0	+0.63+0 j	-1.63+0 j	+0.37,+1.43	+0.39,+1.41
0.1	2.0	-	-	+0.31,+1.59	+0.33,+1.57

[a]Re-started approximation.

CHAPTER IV

STABILITY REGION MAPPING

I. INTRODUCTION

An investigation of the effects of variations in one design parameter is illustrated using the root locus technique described in Chapter III. The effects of parameter variations on both the frequency and damping may be obtained directly from the root locus plot. Since it is conceivable that the loci will change for different base points, generalizations concerning these effects as obtained from the root locus should be made only after considerable analysis.

The inability to generalize is a major disadvantage of root locus. Stability region maps provide a more complete analysis of the effects of parameter variations. For the example used in the previous chapter, a two-dimensional stability map completely describes the effects that parameter variations have on transient stability. This example is illustrated at the end of the chapter.

For an nth degree characteristic equation given by Equation (II-1), the effects of simultaneous variations in the x_i and x_j parameters on stability may be represented by a stability region map. A stability region in the x_i, x_j

plane is defined to be the set points, (x_i, x_j), within the plane which will result in the roots of the characteristic equation having negative real parts. The region's boundary is defined as the set of points which will result in at least one root of G having a zero real part and the other roots negative. Stability region maps serve to isolate the region of stability about a given base point. For parametric studies, this provides realistic bounds on the design parameter based on a stability criterion.

Stability region maps may be refined to provide additional information concerning the roots. Lines of constant damping may be constructed within the region using the root movement technique. In addition, information concerning the oscillatory frequencies is available.

A stability region in the x_i, x_j plane encompassing a stable base point, $\vec{P}^0$, may be obtained using the root movement approximation given by Equation (II-11). The method used in obtaining the stability region is to find a point, $\vec{P}^1$, on the boundary where at least one of the roots of G is zero and the other roots are negative. Once a point on the boundary is found, the approximation is used to find other points on the boundary in a manner such that the boundary is traversed.

II. REGION BOUNDARY

The first point on the boundary, $\vec{P}^1$, is found by varying only one parameter. If x_i represents the axis of abscissas, then Δx_j is set to zero and Δx_i is used to vary x_i negatively from its base point value until the boundary or a predetermined limit is found. In the approximation given by Equation (II-11), $\Delta\vec{X}$ contains zeroes everywhere except in the ith position. The ith position of $\Delta\vec{X}$ contains the negative of the step size. Beginning at the base point, the incremental changes in each root are calculated and are used to modify $\vec{\lambda}$. If any of the roots have become positive, then a point near the boundary has been found. However, if the new roots are all negative, then the approximation is used to determine another incremental root change. The above process is repeated until a point on the boundary is found.

The process of finding the first point on the boundary is similar to the modified root locus technique described in Chapter III. The only difference is in where the process is terminated. As in the root locus technique, a variable step size is used where the step size is adjusted according to the criteria established in Chapter III. The first point on the boundary is referred to as $\vec{P}^1$, where

$$\vec{P}^1 = (x_1^0, x_2^0, \cdots, x_i^1, \cdots, x_j^0, \cdots, x_\ell^0) \quad , \qquad \text{(IV-1)}$$

where the superscript, 0, refers to the base point values.

At the point, $\vec{P}^1$, assume that the real part of the kth root vanishes and that the other n-1 roots have negative real parts. The linear approximation at $\vec{P}^1$ is then:

$$\Delta\lambda_1 = -(\partial G/\partial x_i \,/\, \partial G/\partial\lambda)_{\vec{P}_1^1} \Delta x_i - (\partial G/\partial x_j \,/\, \partial G/\partial\lambda)_{\vec{P}_1^1} \Delta x_j \ , \quad \text{(IV-2)}$$

$$\Delta\lambda_2 = -(\partial G/\partial x_i \,/\, \partial G/\partial\lambda)_{\vec{P}_2^1} \Delta x_i - (\partial G/\partial x_j \,/\, \partial G/\partial\lambda)_{\vec{P}_2^1} \Delta x_j \ , \quad \text{(IV-3)}$$

$$\vdots$$

$$\Delta\lambda_k = -(\partial G/\partial x_i \,/\, \partial G/\partial\lambda)_{\vec{P}_k^1} \Delta x_i - (\partial G/\partial x_j \,/\, \partial G/\partial\lambda)_{\vec{P}_k^1} \Delta x_j \ , \quad \text{(IV-4)}$$

$$\vdots$$

$$\Delta\lambda_n = -(\partial G/\partial x_i \,/\, \partial G/\partial\lambda)_{\vec{P}_n^1} \Delta x_i - (\partial G/\partial x_j \,/\, \partial G/\partial\lambda)_{\vec{P}_n^1} \Delta x_j \ , \quad \text{(IV-5)}$$

where

$$\vec{P}_k^1 = (x_1^0, x_2^0, \cdots, x_i^1, \cdots, x_\ell^0, \lambda_k) \ . \quad \text{(IV-6)}$$

Since $\mathrm{Re}(\lambda_k)$ is zero at $\vec{P}^1$, the homogeneous equation for $\mathrm{Re}(\Delta\lambda_k)$ represents a vector in the x_i, x_j plane which is tangent to the boundary at $\vec{P}^1$. By moving along this vector, new points on the boundary may be found where $\mathrm{Re}(\lambda_k)$ remains zero. The objective is to traverse the boundary in a clockwise manner keeping the base point, $\vec{P}^0$, to the right. To achieve this, Equation (IV-4) is rewritten as:

$$\mathrm{Re}(\Delta\lambda_k) = a_1 \Delta x_i + a_2 \Delta x_j \ , \quad \text{(IV-7)}$$

$$\mathrm{Im}(\Delta\lambda_k) = b_1 \Delta x_i + b_2 \Delta x_j \ , \quad \text{(IV-8)}$$

where

$$a_1 = \frac{\mathrm{Re}\left(\frac{\partial G}{\partial x_i}\right)\mathrm{Re}\left(\frac{\partial G}{\partial \lambda}\right) + \mathrm{Im}\left(\frac{\partial G}{\partial x_i}\right)\mathrm{Im}\left(\frac{\partial G}{\partial \lambda}\right)}{\mathrm{Re}\left(\frac{\partial G}{\partial \lambda}\right)^2 + \mathrm{Im}\left(\frac{\partial G}{\partial \lambda}\right)^2}, \qquad \text{(IV-9)}$$

$$a_2 = \frac{\mathrm{Re}\left(\frac{\partial G}{\partial x_j}\right)\mathrm{Re}\left(\frac{\partial G}{\partial \lambda}\right) + \mathrm{Im}\left(\frac{\partial G}{\partial x_j}\right)\mathrm{Im}\left(\frac{\partial G}{\partial \lambda}\right)}{\mathrm{Re}\left(\frac{\partial G}{\partial \lambda}\right)^2 + \mathrm{Im}\left(\frac{\partial G}{\partial \lambda}\right)^2}, \qquad \text{(IV-10)}$$

$$b_1 = \frac{\mathrm{Im}\left(\frac{\partial G}{\partial x_i}\right)\mathrm{Re}\left(\frac{\partial G}{\partial \lambda}\right) - \mathrm{Re}\left(\frac{\partial G}{\partial x_i}\right)\mathrm{Im}\left(\frac{\partial G}{\partial \lambda}\right)}{\mathrm{Re}\left(\frac{\partial G}{\partial \lambda}\right)^2 + \mathrm{Im}\left(\frac{\partial G}{\partial \lambda}\right)^2}, \qquad \text{(IV-11)}$$

$$b_2 = \frac{\mathrm{Im}\left(\frac{\partial G}{\partial x_j}\right)\mathrm{Re}\left(\frac{\partial G}{\partial \lambda}\right) - \mathrm{Re}\left(\frac{\partial G}{\partial x_j}\right)\mathrm{Im}\left(\frac{\partial G}{\partial \lambda}\right)}{\mathrm{Re}\left(\frac{\partial G}{\partial \lambda}\right)^2 + \mathrm{Im}\left(\frac{\partial G}{\partial \lambda}\right)^2}, \qquad \text{(IV-12)}$$

where all partial derivatives are evaluated at $\vec{P}_k^1$. From the point, $\vec{P}^1$, a second point on the boundary, $\vec{P}^2$, may be found by moving along the tangent vector given above by Equation (IV-7). From $\vec{P}^1$, $\vec{P}^2$ is determined by letting either Δx_i or Δx_j in Equation (IV-7) equal the step size and then solving for the other ΔX required to satisfy the homogeneous equation.

The slope of the tangent line is used to determine which ΔX term is to be solved for. If in the x_i, x_j plane, x_i represents the axis of abscissas, then for tangent lines whose slope magnitude is greater than one, the Δx_j term

should be adjusted by the step size and the Δx_i term should be solved for. The step size may be negative or positive depending upon the direction of travel.

Using the tangent vector corresponding to the zero root, successive points on the boundary are found. At each new point found, the error in the approximation is computed using Equation (III-6). Using the criteria concerning step size adjustment described in Chapter III, the step size may be altered as additional points on the boundary are determined.

Since a stability region may be infinitely large, limits on the design parameters are imposed to restrict the stability region search to a finite area in the x_i, x_j plane. If either parameter exceeds a limit as the boundary is traversed, then the mapping along that direction is discontinued. A new point on the boundary is found by searching along the limit line. By imposing limits on x_i and x_j, the resulting stability region is confined to lie within a rectangle formed by the limit lines.

Example IV-1

To illustrate the method of boundary mapping, consider the following example:

$$G = \lambda^2 + F_1(\vec{X})\lambda + F_0(\vec{X}) = 0 \ , \qquad \text{(IV-13)}$$

where

$$F_1(\vec{X}) = x_1 - x_2 \ , \qquad \text{(IV-14)}$$

$$F_0(\vec{X}) = 0.25(x_1 + x_2) \ , \qquad \text{(IV-15)}$$

$$\vec{X} = (x_1, x_2) \ . \qquad \text{(IV-16)}$$

The base point is given as:

$$\vec{P}^0 = (x_1^0, x_2^0) = (3,2) \ . \qquad \text{(IV-17)}$$

Let x_1 represent the axis of abscissas and x_2 represent the axis of ordinates. Assume that the first point on the boundary, $\vec{P}^1$, has been found using the root locus technique and is given as:

$$\vec{P}^1 = (x_1^1, x_2^0) = (2,2) \ . \qquad \text{(IV-18)}$$

At $\vec{P}^1$, the roots of G are:

$$\lambda_1 = 0 + j \ , \qquad \text{(IV-19)}$$

$$\lambda_2 = 0 - j \ . \qquad \text{(IV-20)}$$

The approximating equation, Equation (II-11), becomes:

$$\Delta\lambda_1 = -\left(\partial G/\partial x_1 \Big/ \partial G/\partial\lambda\right)_{\vec{P}_1^1} \Delta x_1 - \left(\partial G/\partial x_2 \Big/ \partial G/\partial\lambda\right)_{\vec{P}_1^1} \Delta x_2 \ , \qquad \text{(IV-21)}$$

$$\Delta\lambda_2 = -\left(\partial G/\partial x_1 \Big/ \partial G/\partial\lambda\right)_{\vec{P}_2^1} \Delta x_1 - \left(\partial G/\partial x_2 \Big/ \partial G/\partial\lambda\right)_{\vec{P}_2^1} \Delta x_2 \ . \qquad \text{(IV-22)}$$

After evaluating the partial derivatives at $\vec{P}^1$, the above equations become:

$$\Delta\lambda_1 = -\frac{(0.25 + j)}{2j}\Delta x_1 - \frac{(0.25 - j)}{2j}\Delta x_2 , \quad \text{(IV-23)}$$

$$\Delta\lambda_2 = \frac{(0.25 - j)}{2j}\Delta x_1 + \frac{(0.25 + j)}{2j}\Delta x_2 . \quad \text{(IV-24)}$$

Since both λ_1 and λ_2 have a zero real part at $\vec{P}^1$, either equation may be used to determine $\vec{P}^2$. By using the $\Delta\lambda_1$ equation and rewriting, the following equations are obtained:

$$\mathrm{Re}(\Delta\lambda_1) = -0.5\Delta x_1 + 0.5\Delta x_2 , \quad \text{(IV-25)}$$

$$\mathrm{Im}(\Delta\lambda_1) = 0.125\Delta x_1 + 0.125\Delta x_2 . \quad \text{(IV-26)}$$

Requiring that $\mathrm{Re}(\Delta\lambda_1) = 0$, Equation (IV-25) represents a vector tangent to the boundary at $\vec{P}^1$. Since the slope of the tangent vector is one, let Δx_2 equal the step size of 0.1 and solve for Δx_1. This may be summarized as follows:

$$\mathrm{Re}(\Delta\lambda_1) = -0.5\Delta x_1 + 0.5\Delta x_2 = 0 , \quad \text{(IV-27)}$$

$$\Delta x_1 = \Delta x_2 = 0.1 . \quad \text{(IV-28)}$$

This defines a new point on the boundary as:

$$\vec{P}^2 = (x_1^2, x_2^2) = (2.1, 2.1) . \quad \text{(IV-29)}$$

The approximated roots at $\vec{P}^2$ are determined by:

$$\vec{\lambda}^2 = \vec{\lambda}^1 + \Delta\vec{\lambda}^1 \ , \qquad \text{(IV-30)}$$

where $\Delta\vec{\lambda}^1$ is determined using the $\Delta\vec{X}$ given by Equation (IV-28). The approximated roots at $\vec{P}^2$ are then:

$$\lambda_1 = 0 + 1.025j \ , \qquad \text{(IV-31)}$$

$$\lambda_2 = 0 - 1.025j \ . \qquad \text{(IV-32)}$$

The error estimate at $\vec{P}^2$ may be computed as follows:

$$\text{error} = \left| \lambda_1^2 \, \lambda_2^2 - F_0(\vec{X}) \right|$$

$$\text{error} = \left| (1.025)(1.025) - 1.05 \right| = 0 \ . \qquad \text{(IV-33)}$$

Beginning at $\vec{P}^2$, additional points may be found by repeating this process. If the computed error estimate at any point is determined to be larger than 0.1, then G is re-solved to provide a new starting point.

Figure 3 is the stability region computed for this example using the method of tangent vectors. At the point, (5,5), the search along the upper boundary was terminated and a new point on the boundary was found at (5,-5) by searching along the x_1 limit line, $x_1 = 5$. Table III summarizes the computations used in obtaining Figure 3.

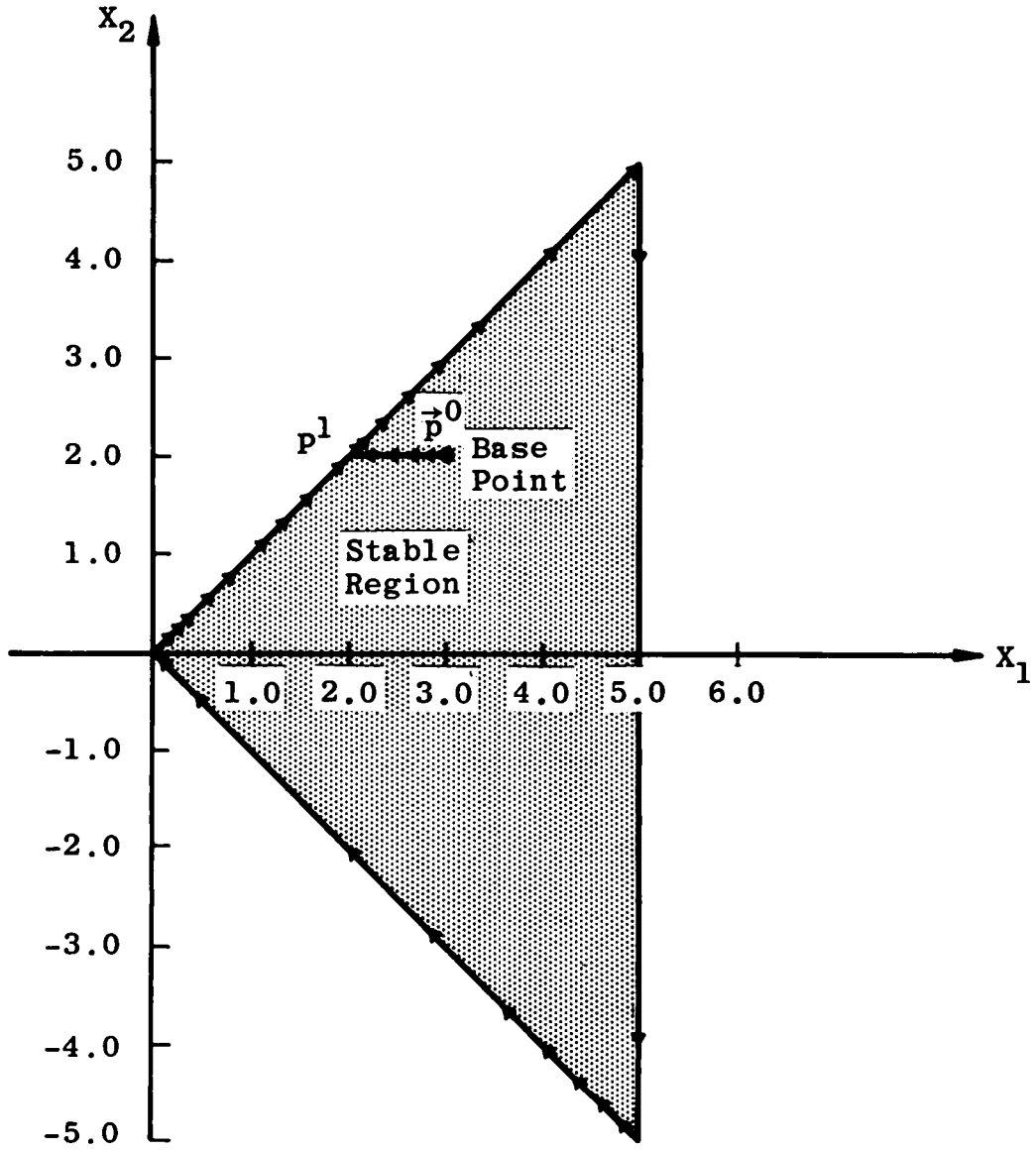


Figure 3. Stability region map for example IV-1.

TABLE III

SUMMARY OF COMPUTATIONS USED IN OBTAINING FIGURE 3

x_1	x_2	Tangent Vector(λ_1)	Tangent Vector(λ_2)	Approximate Roots	Actual Roots
2.0	2.0	$(-0.5\ \Delta x_1+0.5\ \Delta x_2)$	$(-0.5\ \Delta x_1+0.5\ \Delta x_2)$	-	$0 \pm 1\ j$
2.1	2.1	$(-0.5\ \Delta x_1+0.51\ \Delta x_2)$	$(-0.51\Delta x_1+0.51\Delta x_2)$	$0 \pm 1.025j$	$0 \pm 1.024j$
2.2	2.2	$(-0.501\Delta x_1+0.501\Delta x_2)$	$(-0.5\ \Delta x_1+0.5\ \Delta x_2)$	$0 \pm 1.05\ j$	$0 \pm 1.048j$
2.4	2.4	$(-0.5\ \Delta x_1+0.5\ \Delta x_2)$	$(-0.5\ \Delta x_1+0.5\ \Delta x_2)$	$0 \pm 1.1\ j$	$0 \pm 1.09\ j$
2.6	2.6	$(-0.5\ \Delta x_1+0.5\ \Delta x_2)$	$(-0.5\ \Delta x_1+0.5\ \Delta x_2)$	$0 \pm 1.15\ j$	$0 \pm 1.14\ j$
3.0	3.0	$(-0.5\ \Delta x_1+0.5\ \Delta x_2)$	$(-0.5\ \Delta x_1+0.5\ \Delta x_2)$	$0 \pm 1.24\ j$	$0 \pm 1.22\ j$
3.4	3.4	$(-0.5\ \Delta x_1+0.5\ \Delta x_2)$	$(-0.5\ \Delta x_1+0.5\ \Delta x_2)$	$0 \pm 1.32\ j$	$0 \pm 1.3\ j$
4.2	4.2	$(-0.5\ \Delta x_1+0.5\ \Delta x_2)$	$(-0.5\ \Delta x_1+0.5\ \Delta x_2)$	$0 \pm 1.47\ j$	$0 \pm 1.48\ j$
5.0	5.0	-	-	$0 \pm 1.61\ j$	$0 \pm 1.58\ j$
5.0	-5.0	$(-\Delta x_1-\Delta x_2)$	$(-0.98\Delta x_1+1.03\Delta x_2)$	-	$0,-10.0$
4.9	-4.9	$(-\Delta x_1-\Delta x_2)$	$(-0.98\Delta x_1+1.03\Delta x_2)$	$0,-9.8$	$0,-9.8$
4.8	-4.8	$(-\Delta x_1-\Delta x_2)$	$(-0.98\Delta x_1+1.01\Delta x_2)$	$0,-9.6$	$0,-9.6$

TABLE III (continued)

x_1	x_2	Tangent Vector(λ_1)	Tangent Vector(λ_2)	Approxi-mate Roots	Actual Roots
4.6	-4.6	$(-\Delta x_1-\Delta x_2)$	$(-0.98\Delta x_1+1.02\Delta x_2)$	0,-9.2	0,- 9.2
4.4	-4.4	$(-\Delta x_1-\Delta x_2)$	$(-0.97\Delta x_1+1.03\Delta x_2)$	0,-8.8	0,- 8.8
4.0	-4.0	$(-\Delta x_1-\Delta x_2)$	$(-0.97\Delta x_1+1.03\Delta x_2)$	0,-8.0	0,- 8.0
3.6	-3.6	$(-\Delta x_1-\Delta x_2)$	$(-0.97\Delta x_1+1.03\Delta x_2)$	0,-7.2	0,- 7.2
2.6	-2.6	$(-\Delta x_1-\Delta x_2)$	$(-0.96\Delta x_1+1.04\Delta x_2)$	0,-5.6	0,- 5.6
1.8	-1.8	$(-\Delta x_1-\Delta x_2)$	$(-0.93\Delta x_1+1.07\Delta x_2)$	0,-3.6	0,- 3.6
1.4	-1.4	$(-\Delta x_1-\Delta x_2)$	$(-0.91\Delta x_1+1.09\Delta x_2)$	0,-2.8	0,- 2.8
1.0	-1.0	$(-\Delta x_1-\Delta x_2)$	$(-0.88\Delta x_1+1.12\Delta x_2)$	0,-2.0	0,- 2.0
0.6	-0.6	$(-\Delta x_1-\Delta x_2)$	$(-0.79\Delta x_1+1.21\Delta x_2)$	0,-1.2	0,- 1.2
0.2	-0.2	$(-\Delta x_1-\Delta x_2)$	$(-0.37\Delta x_1+1.63\Delta x_2)$	0,-0.4	0,- 0.2
0.1	-0.1	$(-\Delta x_1-\Delta x_2)$	$(-0.25\Delta x_1+2.25\Delta x_2)$	0,-0.2	0,- 0.2

TABLE III (continued)

x_1	x_2	Tangent Vector(λ_1)	Tangent Vector(λ_2)	Approximate Roots	Actual Roots
0.05	0.05	$(-0.5\ \Delta x_1 + 0.5\ \Delta x_2)$	$(-0.5\ \Delta x_1 + 0.5\ \Delta x_2)$	-	$0 \pm 0.316j$
0.15	0.15	$(-0.5\ \Delta x_1 + 0.5\ \Delta x_2)$	$(-0.5\ \Delta x_1 + 0.5\ \Delta x_2)$	$0 \pm 0.394j$	$0 \pm 0.34\ j$
0.25	0.25	$(-0.5\ \Delta x_1 + 0.5\ \Delta x_2)$	$(-0.5\ \Delta x_1 + 0.5\ \Delta x_2)$	$0 \pm 0.46\ j$	$0 \pm 0.41\ j$
1.15	1.15	$(-0.5\ \Delta x_1 + 0.5\ \Delta x_2)$	$(-0.5\ \Delta x_1 + 0.5\ \Delta x_2)$	-	$0 \pm 0.75\ j$

III. REGION CHARACTERISTICS

The stability region's boundary was defined to be the set of points within the plane where at least one root of the characteristic equation is zero and all other roots are negative. Within the stability region, the roots behave in a manner predictable by the tangent vectors. Lines of constant damping, constant λ, and constant frequency may be constructed. For a parametric study of a system containing two design parameters, a two-dimensional stability region map completely describes the effects of parameter variations.

To illustrate the information which can be obtained concerning the stability region, consider the previous example. As indicated in Table III, the tangent vectors coincide along the upper boundary. This could be expected since both roots have a zero real part along this part of the boundary. On the lower boundary however, the tangent vectors are not equal and only the vector corresponding to the zero root is used to map the boundary. By using the vector corresponding to the non-zero root, other points within the region may be obtained which yield no change in the non-zero root. For example, at the point, (1,-1), the non-zero root is

$$\lambda_2 = -2.0 \ . \qquad \text{(IV-34)}$$

The corresponding tangent vector is

$$Re(\Delta\lambda_2) = - 0.88\Delta x_1 + 1.12\Delta x_2 \ . \qquad \text{(IV-35)}$$

Requiring that $Re(\Delta\lambda_2)$ equal zero and that $Re(\Delta\lambda_1)$ be negative will yield a point within the region where λ_2 remains -2.0. Continuing along using the tangent vector for λ_2, additional points may be obtained where λ_2 is a constant -2.0. Similarly, constant λ lines for different λ's may be constructed.

Figure 4 is a detailed stability map for Example IV-1 showing the construction of several constant λ lines throughout the region. It is interesting to note that each constant λ line is tangent to a parabola which corresponds to zero frequency. The parabola consists of multiple roots and serves to separate the stability region into two areas. The area bounded above by the region's upper boundary and below by the multiple root parabola contains points where the roots are complex. The area bounded above by the multiple root parabola and below by the region's lower boundary contains points where the roots are real.

The shaded area shown in Figure 4 contains those points within the region where the roots are complex. Within the complex zone, lines of constant damping may be constructed using the tangent vectors. For example, at the initial base point, (3,2), the roots are:

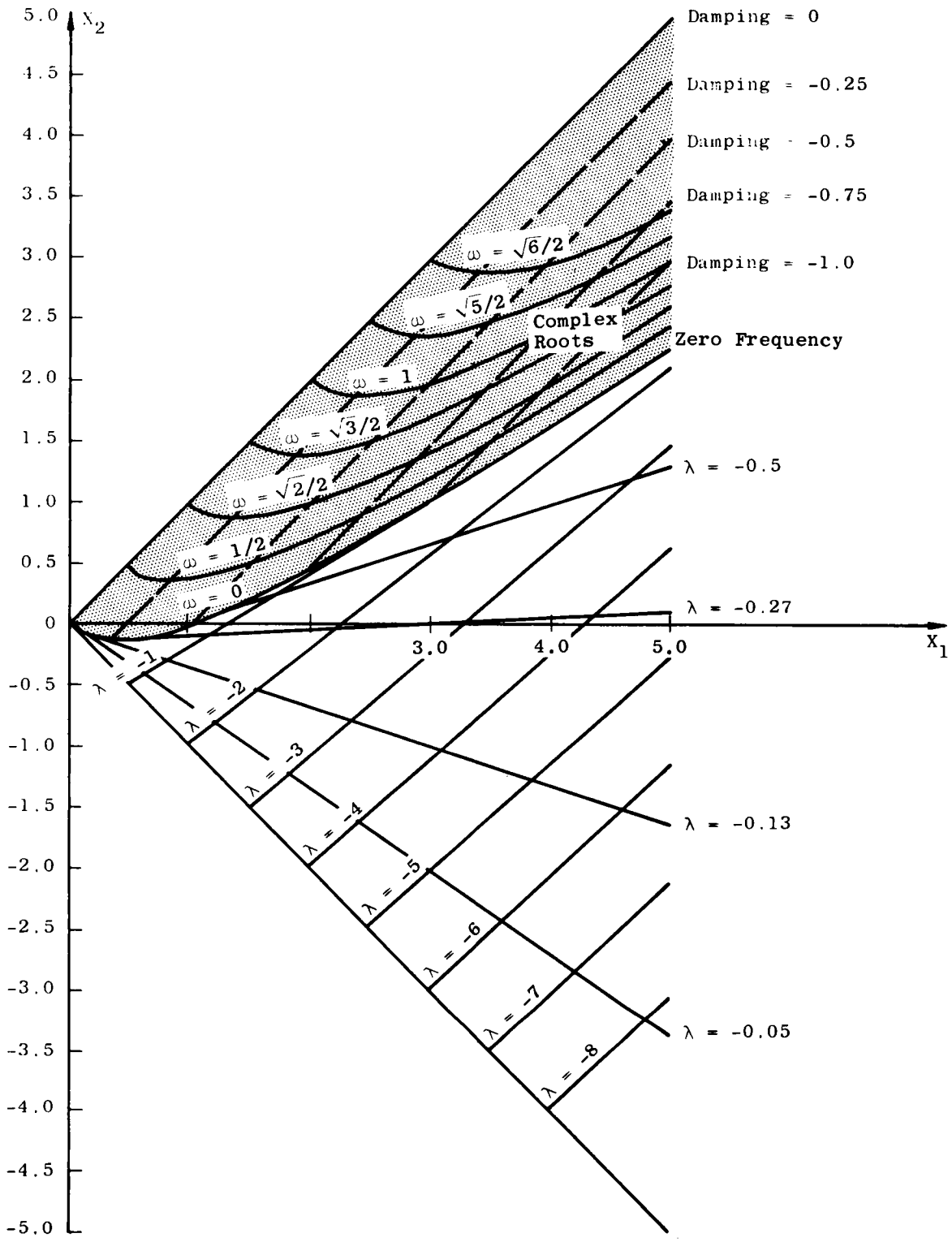


Figure 4. Detailed stability region map for example IV-1.

$$\lambda_1 = -0.5 + j \ , \qquad \text{(IV-36)}$$

$$\lambda_2 = -0.5 - j \ . \qquad \text{(IV-37)}$$

The corresponding tangent vectors are:

$$\Delta\lambda_1 = (0.5+0.125j)\Delta x_1 + (-0.5-0.375j)\Delta x_2 \ , \qquad \text{(IV-38)}$$

$$\Delta\lambda_2 = (0.5-0.125j)\Delta x_1 + (-0.5+0.375j)\Delta x_2 \ . \qquad \text{(IV-39)}$$

Since the real parts of λ_1 and λ_2 are equal, either equation may be used. Using Equation (IV-38) and rewriting gives:

$$\mathrm{Re}(\Delta\lambda_1) = 0.5\Delta x_1 = 0.5\Delta x_2 \ . \qquad \text{(IV-40)}$$

Requiring Equation (IV-40) to be zero will yield other points within the region where the real part of λ_1 and λ_2 is -0.5. Figure 4 shows several lines of constant damping which were constructed using the tangent vectors. The lines of constant frequency were constructed using a tangent vector corresponding to the imaginary part of Equation (IV-38). For example, at the point, (3,2),

$$\mathrm{Im}(\Delta\lambda_1) = 0.125\Delta x_1 - 0.375\Delta x_2 \ . \qquad \text{(IV-41)}$$

Requiring Equation (IV-41) to be zero will yield other points where the complex part of λ remains constant.

IV. THREE-DIMENSIONAL REGIONS

Two-dimensional stability regions were determined by permitting only two design parameters to vary. Three-dimensional maps can be obtained by generating a series of two-dimensional maps for different values of a third parameter. The map obtained in this manner consists of a series of contour curves and is just a repetition of the two-dimensional process.

CHAPTER V

EFFECTS OF PARAMETER VARIATIONS ON AIRCRAFT LATERAL STABILITY

I. INTRODUCTION

The equations of motion governing an aircraft may be linearized such that they form two independent sets of equations pertaining to longitudinal and lateral motion [4]. The linearized equations are ordinary linear homogeneous differential equations whose coefficients are functions of various aerodynamic and inertia factors. As mentioned previously, the solution to such a set of equations is exponential and an investigation of stability can be performed by analyzing the eigenvalues of the coefficient matrix.

A computer program using the root movement technique has been written to investigate the effects of variations in the aerodynamic factors on the lateral stability characteristics. The characteristic equation which is used [5] is in body axis and is of the form:

$$G = \lambda^4+F_3(\vec{X})\lambda^3+F_2(\vec{X})\lambda^2+F_1(\vec{X})\lambda+F_0(\vec{X}) \quad , \qquad \text{(V-1)}$$

where

$$\vec{X} = (C_{Y_\beta}, C_{Y_p}, C_{Y_r}, C_{\ell_\beta}, C_{\ell_p}, C_{\ell_r}, C_{n_\beta}, C_{n_p}, C_{n_r}) \quad . \qquad \text{(V-2)}$$

The exact form of the characteristic equation used is given in Appendix II.

II. PROGRAM DESCRIPTION

A generalized flow chart of the computer program is illustrated in Figure 5. As can be seen in the flow chart, the input base point data can be in either stability or body axis form. If the input derivative data is in stability axis, then it is converted to body axis form [6]. All output data from the program is with reference to the body axis.

The system of approximating equations relating the movement of the roots as a function of changes in the design parameters was developed in Chapter II and was given as:

$$\Delta\vec{\lambda} = A\Delta\vec{X} \ . \qquad \text{(V-3)}$$

The roots of G at the nth point are determined using Equation (V-3) and are given as:

$$\vec{\lambda}^{n} = \vec{\lambda}^{n-1} + A\Big|_{n-1} \Delta\vec{X} \ , \qquad \text{(V-4)}$$

where the elements of A are evaluated at the n-1 point. In the lateral stability program, $\vec{\lambda}^{n}$ and $\vec{\lambda}^{n-1}$ are four component column vectors, A is a 4x9 matrix whose elements are given by Equation (II-10), and $\Delta\vec{X}$ is a nine-component column vector.

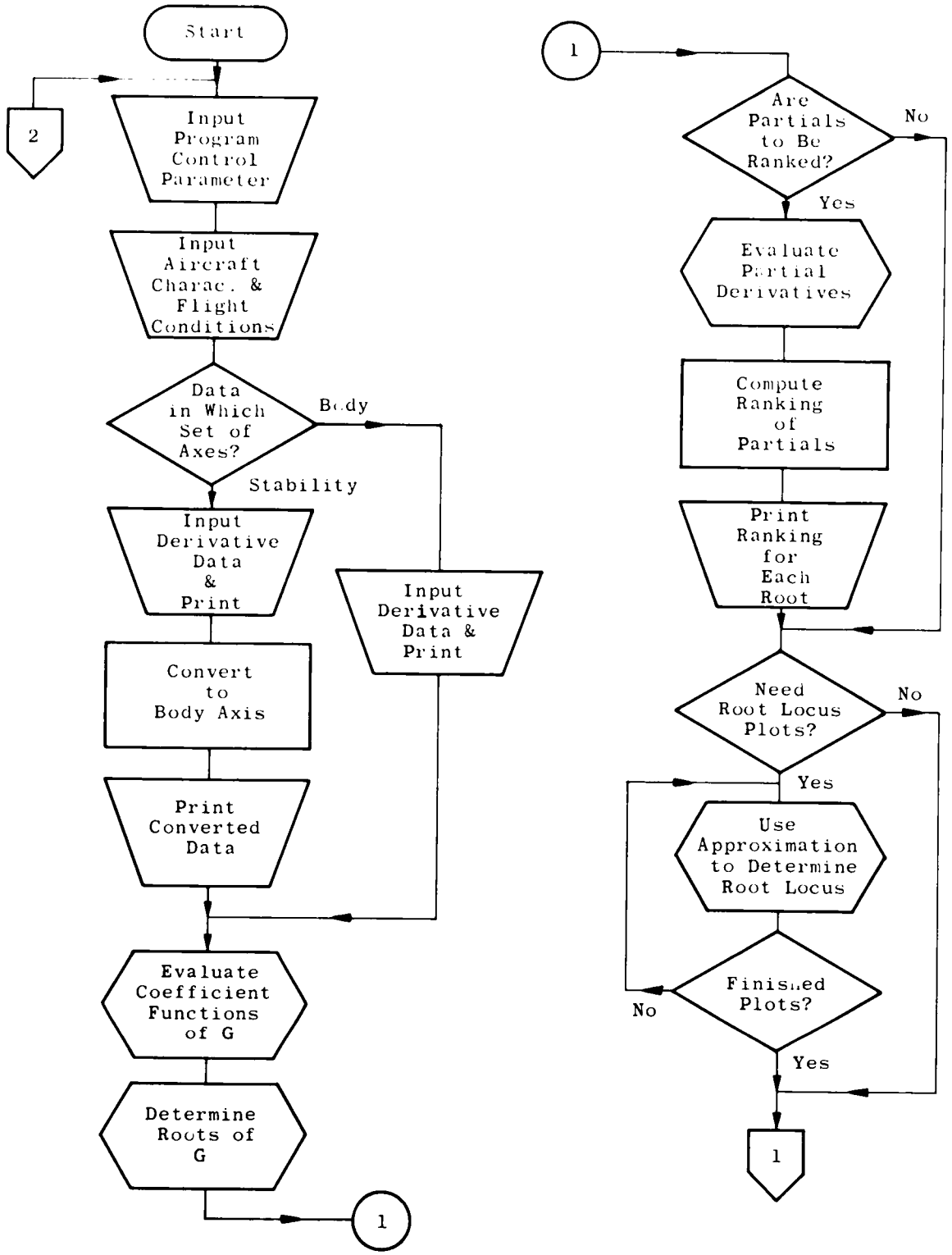


Figure 5. Basic flow chart for lateral stability investigation computer program.

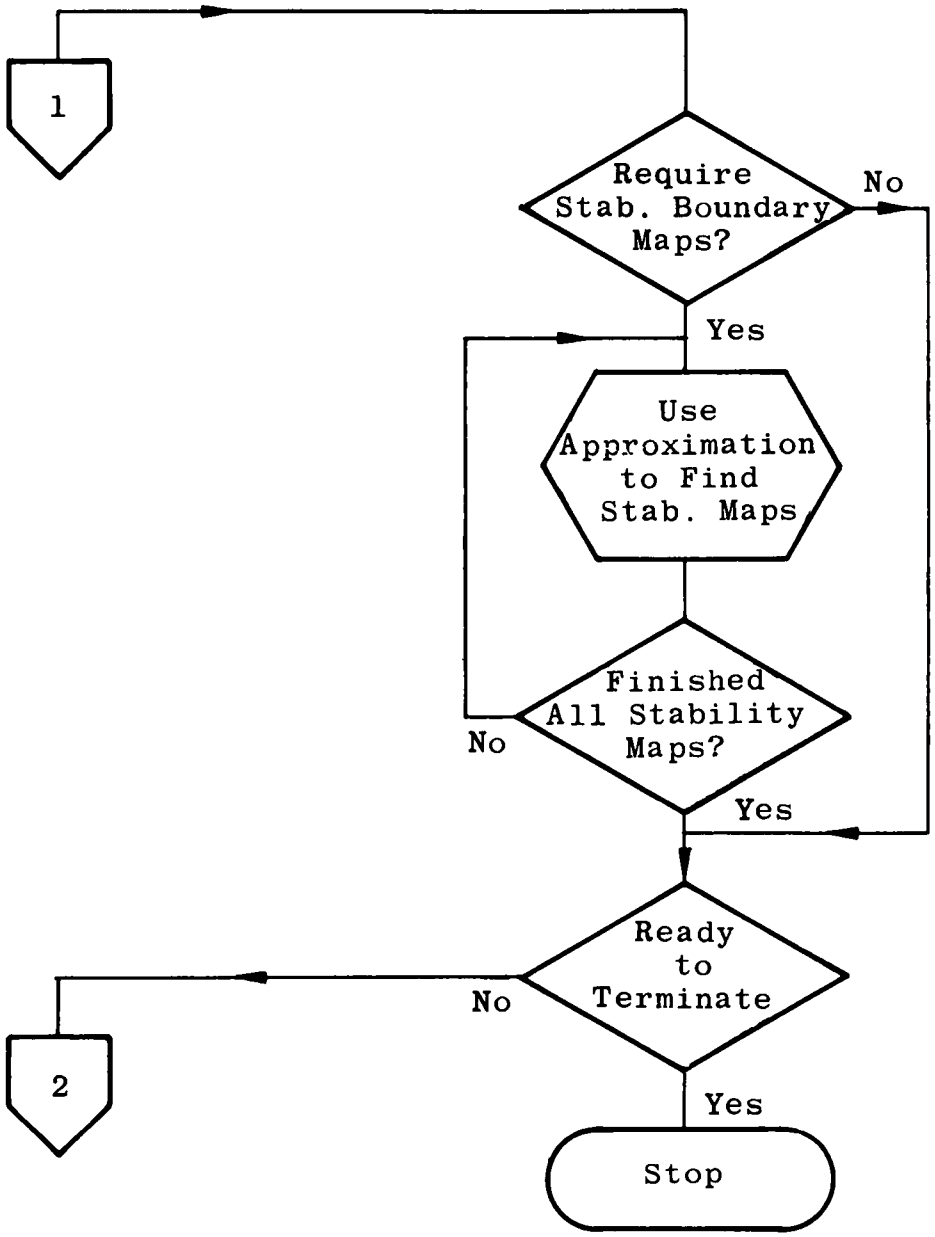


Figure 5. (continued)

Root Locus

The effects of parameter variations of any element in $\vec{X}$ are accomplished using the modified root locus technique described in Chapter III. If this option is elected, then the necessary information concerning the aerodynamic term to be investigated is read in from the root locus subroutine, RLOCUS. A detailed flow chart of subroutine RLOCUS is illustrated in Figure 6.

In the root locus routine, only one parameter is to be investigated and hence, there is only one non-zero element in the vector, $\Delta\vec{X}$. The sparseness of the $\Delta\vec{X}$ vector enables one to investigate only the appropriate column of the matrix, A. For example, if the third element of $\vec{X}$ is to be investigated, then $\Delta\vec{X}$ contains zeroes in all positions except the third. This requires that only the third column of A be evaluated for such an investigation and eliminates a considerable number of useless computations.

The computer output from the root locus investigation is the value of the roots at prescribed increments of the parameter. The increment at which to print is controlled from the root locus control card. If the initial base point is stable, then the value of the parameter and the roots is printed at the first point of instability. This message is printed regardless of the print control parameter. In addition to the tabulated data, the program has a printer plot routine which provides a graphical

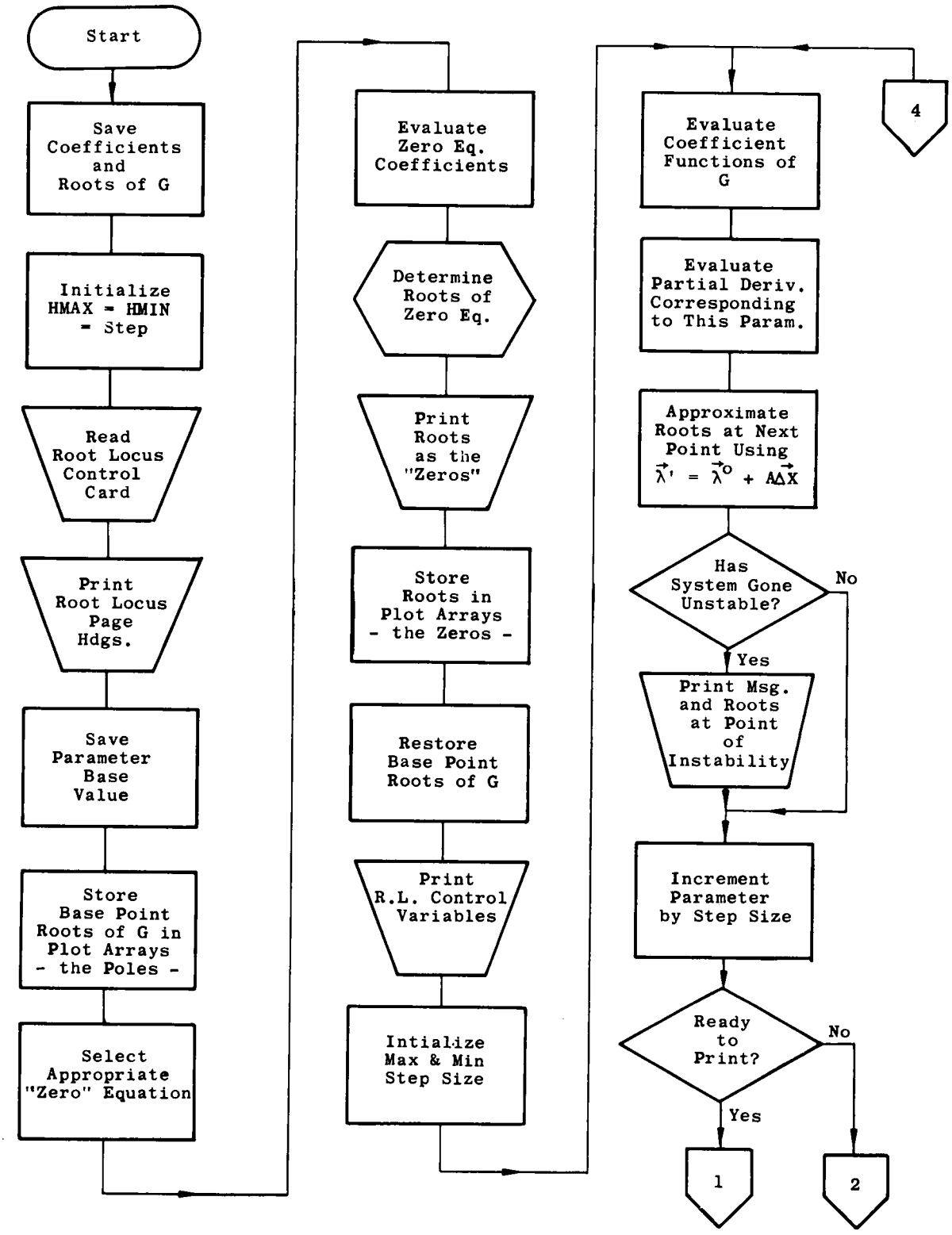


Figure 6. Flow diagram of root locus subroutine.

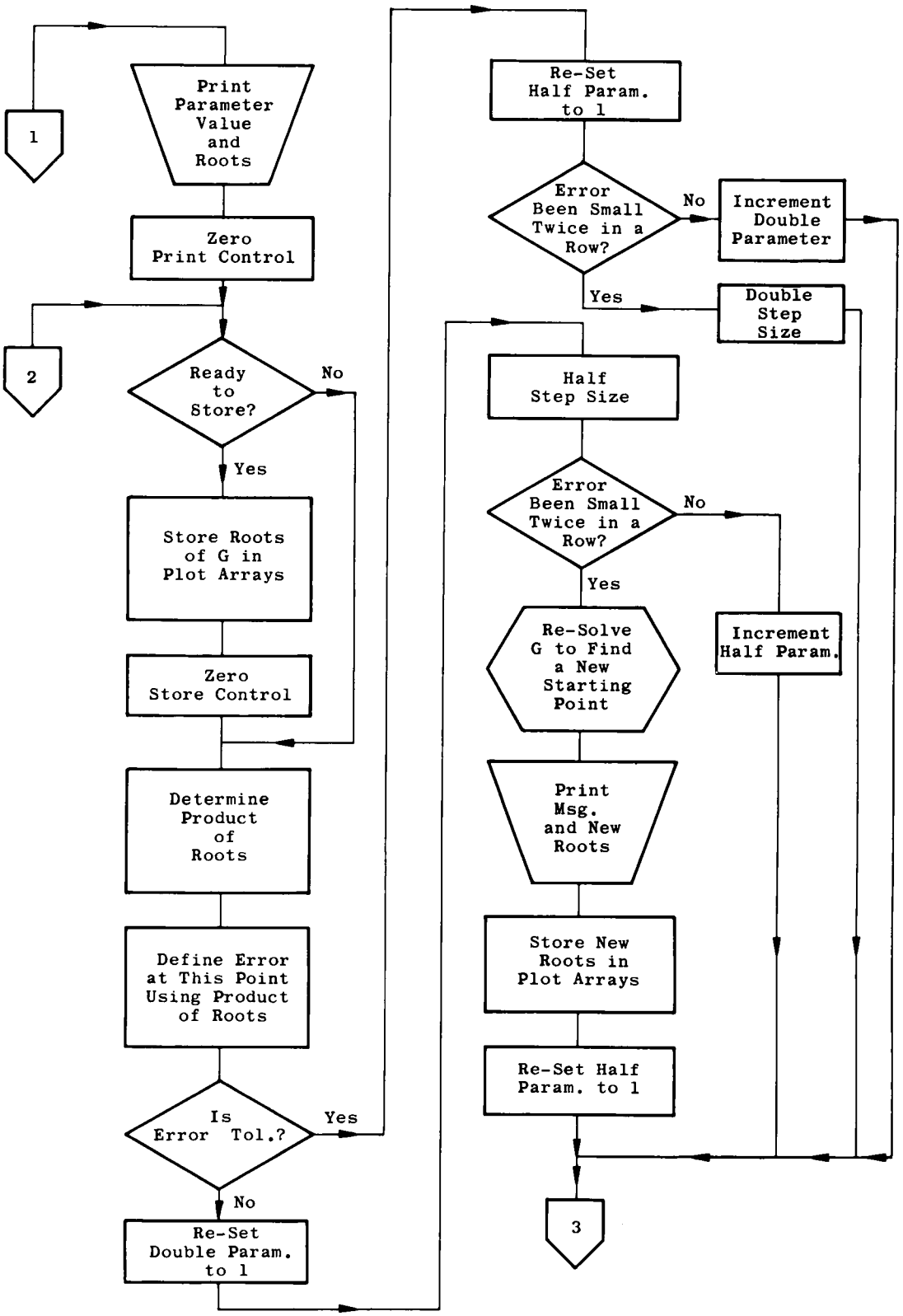


Figure 6. (continued)

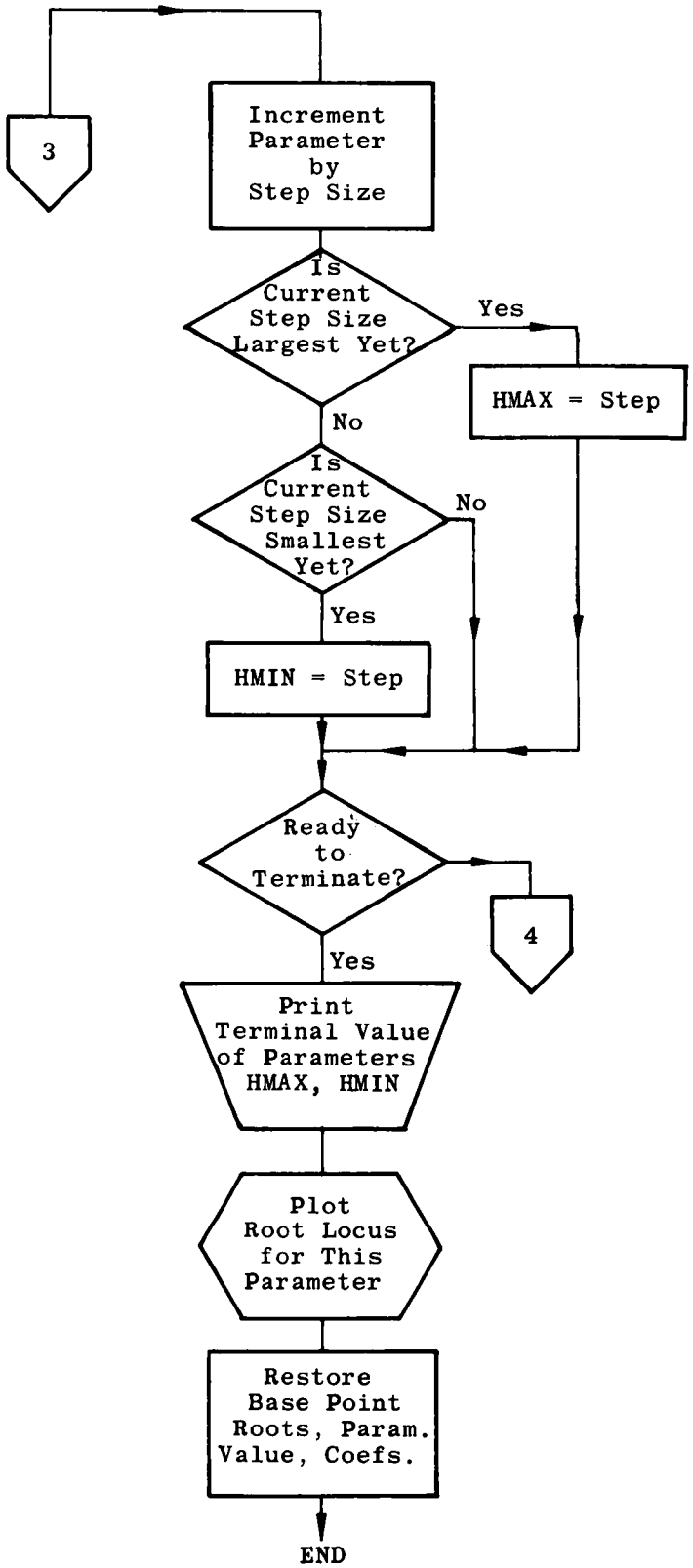


Figure 6. (continued)

display of the movement of the roots in the complex plane. A separate input control parameter is used to control the increment at which the roots are to be stored for plotting.

In addition to tabulating and plotting the roots at specified increments of the design parameter, the form of the zero equation and its roots are tabulated. The zero equations for each of the nine aerodynamic terms are obtained by applying Equation (III-1) to Equation (V-1) and are given in Appendix II.

Stability Region Mapping

Two-dimensional stability region maps can be obtained using the procedure described in Chapter IV. As mentioned previously, a point on the boundary is defined to be a point in the x_i, x_j plane where at least one of the roots of the characteristic equation has a zero real part. Corresponding to each zero root, there exists a tangent vector of the form

$$\mathrm{Re}(\Delta\lambda_k) = a_1\Delta x_i + a_2\Delta x_j \ . \qquad \text{(V-5)}$$

Requiring Equation (V-5) to equal zero will yield another point in the x_i, x_j plane where λ_k remains zero. In Equation (V-5), Δx_i and Δx_j are unknowns and a_1, a_2 are computed using Equations (IV-9) and (IV-10). Since Equation (V-5) has two unknowns, it is necessary to specify one and then solve for the other. The quantity specified is

referred to as the step size. To determine which ΔX term in Equation (V-5) is to be specified and which is to be solved for, it is necessary to examine the possibilities which may occur at a boundary point. Figure 7 illustrates the possibilities which exist. In addition to knowing the tangent vector slope, it is necessary to know the required travel direction. The direction of travel is always such that the stable region is to the right of the directed line segment, $\vec{PP}_1$. In Figure 7 the direction of travel is shown to be positive for each possibility, where positive travel is defined to be the direction of increasing ordinate values. For negative travel, the stable zone would be opposite that pictured.

The solution to Equation (V-5) then provides a new point, $\vec{P}^1$ on the boundary. At $\vec{P}^1$, the error in the roots is determined using Equation (III-6). If the error is excessive, then Equation (V-1) is re-solved and the step size is halved.

If only one root has a zero real part at the boundary point, then its corresponding tangent vector is used to determine a neighboring point where the root remains zero. However, if more than one root is zero, then the various possibilities which arise must be analyzed and the proper tangent vector selected. Note that for a pair of complex roots with zero real part that the corresponding

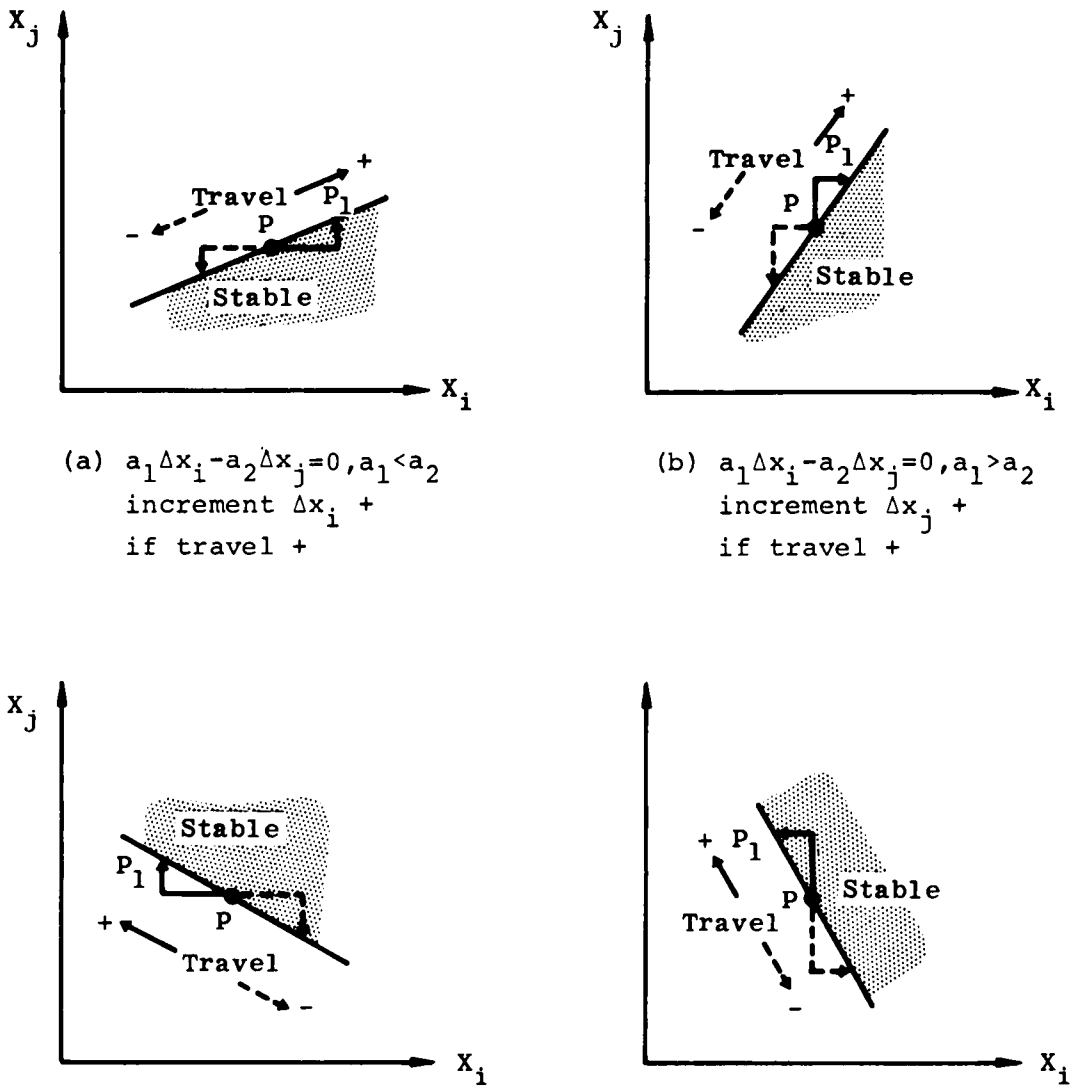
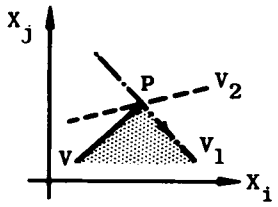


Figure 7. Tangent vector possibilities.

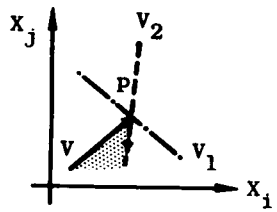
real tangent vectors are equal and hence, there is only one equivalent tangent vector.

If at a boundary point there are two different tangent vectors corresponding to zero roots, then the possibilities may be divided into two classifications according to slope signs. If the two tangent vectors have opposite slope signs, then the correct vector and travel direction may be determined by examining the magnitude of the slopes. The various possibilities which exist are illustrated in Figure 8. Similarly, if the two tangent vectors have the same slope signs, the correct vector and travel direction may be determined by examining the slope magnitudes. Figure 9 illustrates the various possibilities which exist for this case. It can be seen that for the dual direction possibilities, the problem of determining the correct tangent vector corresponds to selecting the vector which is to the right of the last movement on the boundary. In both Figures 8 and 9, V represents the last tangent vector traveled. At the point, $\vec{P}^1$, the two possible vectors are denoted V_1 and V_2. The shaded area represents the stable part of the region.

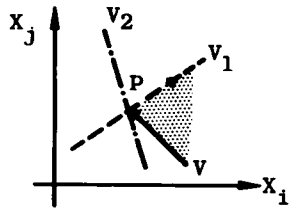
For an arbitrary shaped region, points on the boundary may be found where the tangent vector undergoes a change in slope signs. At such corner points, it is necessary to explore the region about the point to determine the correct travel direction. Figure 10 illustrates the



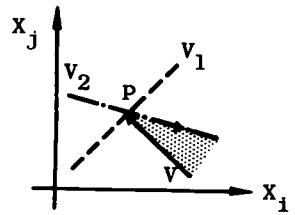
(a) V_2 slope < V slope, travel V_1 negatively



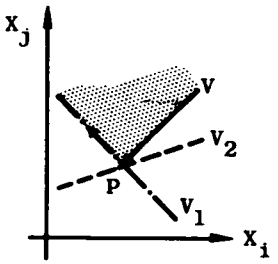
(b) V_2 slope > V slope, travel V_2 negatively



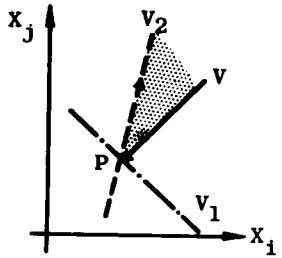
(c) V_2 slope > V slope, travel V_1 positively



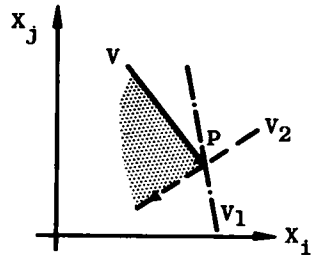
(d) V_2 slope < V slope, travel V_2 negatively



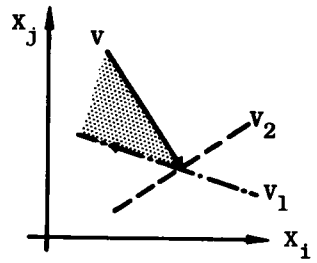
(e) V_2 slope < V slope, travel V_1 positively



(f) V_2 slope > V slope, travel V_2 positively

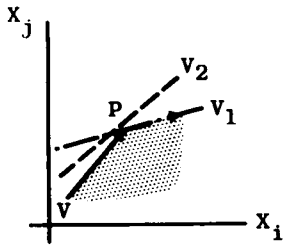


(g) V_1 slope > V slope, travel V_2 negatively

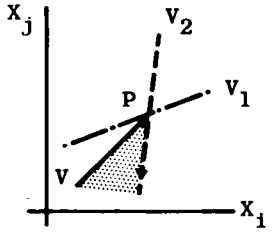


(h) V_1 slope < V slope, travel V_1 positively

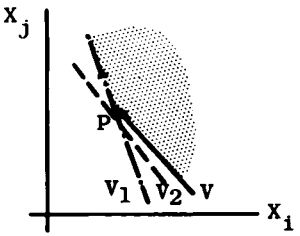
Figure 8. Dual direction possibilities, opposite slope signs.



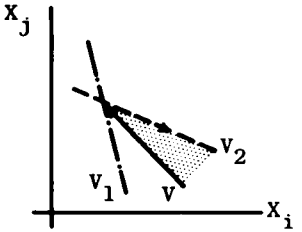
(a) V_1 slope < V_2 slope < V slope → use V_1 positively



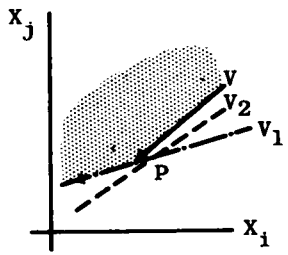
(b) V_1 slope < V slope < V_2 slope → use V_2 negatively



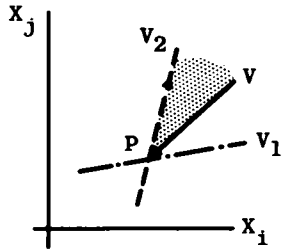
(c) V slope < V_2 slope < V_1 slope → use V_1 positively



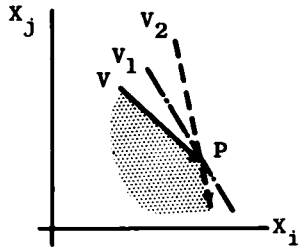
(d) V_2 slope < V slope < V_1 slope → use V_2 negatively



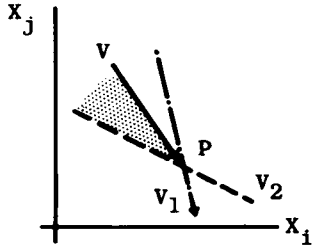
(e) V_1 slope < V_2 slope < V slope → use V_1 negatively



(f) V_1 slope < V slope < V_2 slope → use V_2 positively



(g) V slope < V_1 slope < V_2 slope → use V_2 negatively



(h) V_2 slope < V slope < V_1 slope → use V_2 positively

Figure 9. Dual direction possibilities, same slope signs.

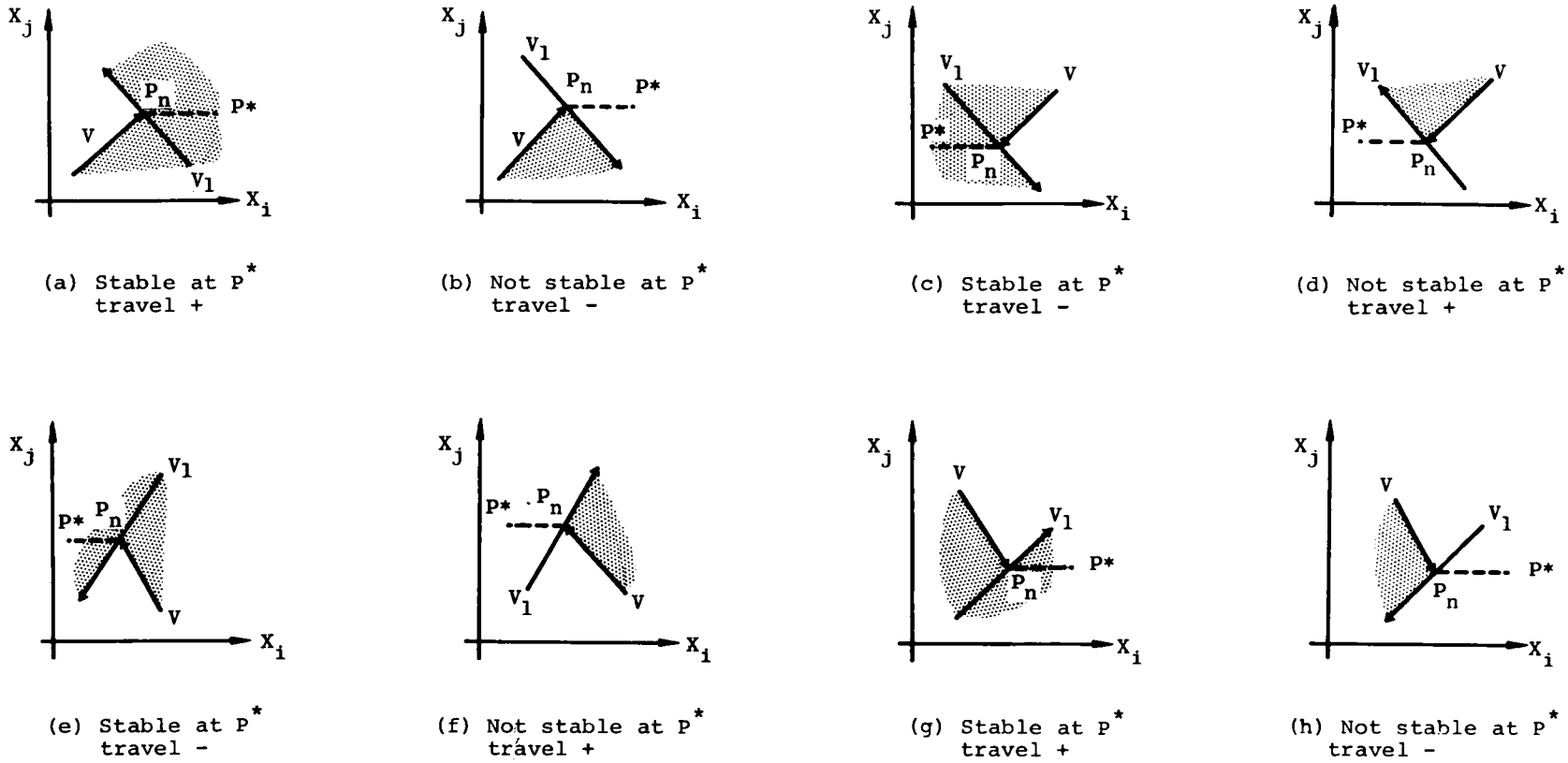


Figure 10. Corner point tangent vector possibilities.

various corner point possibilities. In Figure 10, V represents the last vector traveled, $\vec{P}^n$ represents the corner point, V_1 represents the tangent vector corresponding to the zero root at point $\vec{P}^n$, and P^* represents an exploratory point. At P^*, the characteristic equation is solved to determine system stability. Using the information acquired at the exploratory point, the correct travel direction along V_1 is computed.

The stability region boundary was defined to be the set of points in the x_i, x_j plane where at least one of the roots of the characteristic equation has a zero real part. In actual practice, the defining roots are required only to be near zero. Hence, the set of points computed as the boundary lies within a band about the true boundary. Figure 11 illustrates an arbitrary region where the true boundary is indicated by the solid curve. The broken curves indicate the boundary zone.

It is possible in traversing the boundary to lose contact with the boundary zone. For example, at point P_i in Figure 11, the tangent vector is denoted by V. Using the tangent vector, a point, P^*, is determined which is found to lie outside the boundary zone. By re-setting to point P_i and decreasing the step size, a point, P_{i+1}, can be found which does lie within the boundary zone.

Since stability regions may extend to infinity, realistic limits must be imposed on the region which is to

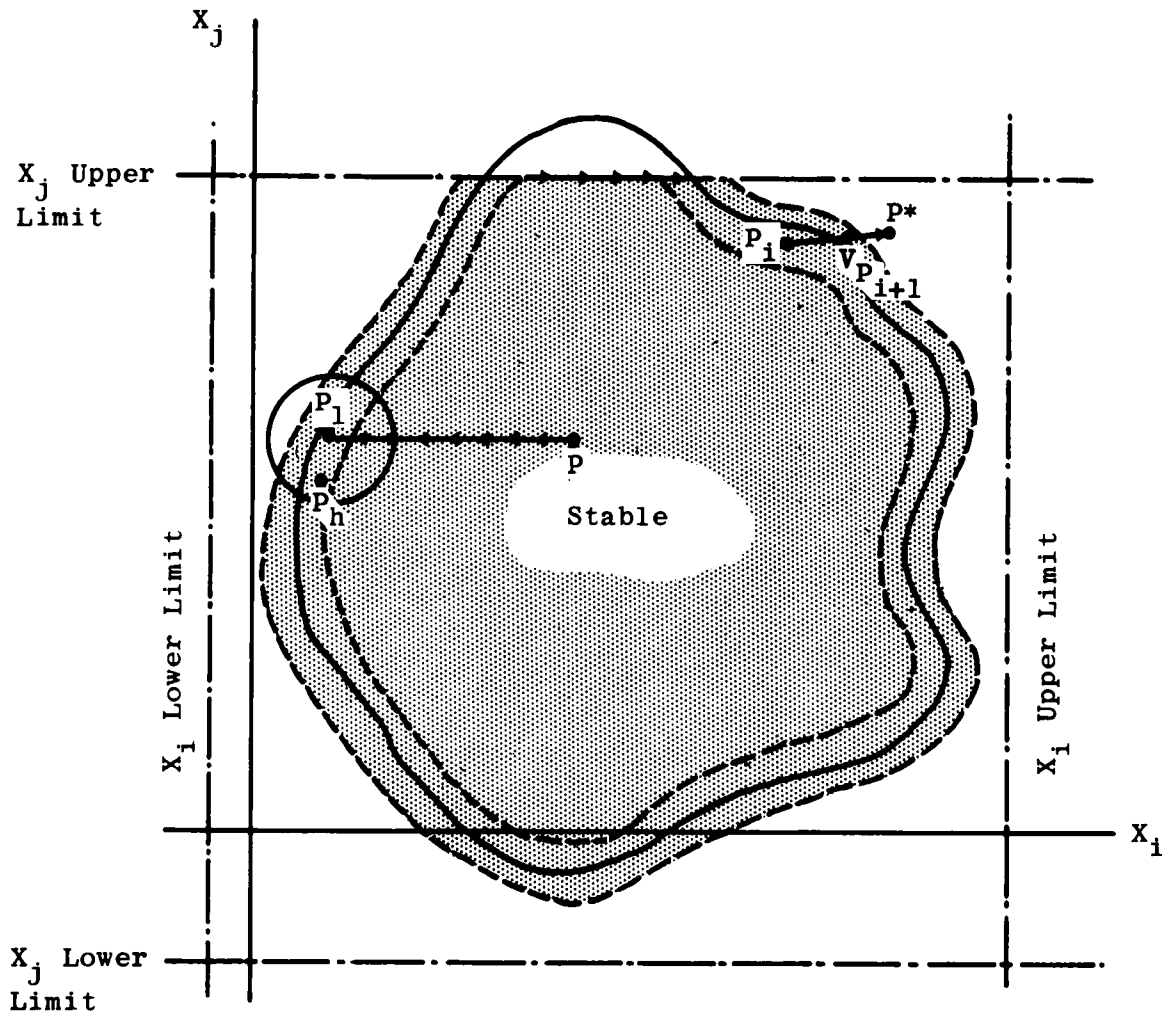


Figure 11. Arbitrary stability region map.

be mapped. If a limit is encountered, the boundary search along the last direction is discontinued and a one-dimensional search is made along the limit line to determine a new point on the boundary. Figure 11 illustrates the procedure which is used when a limit is encountered. The arrowheads indicate the direction of travel.

The boundary mapping is terminated when the perimeter of the region is traversed. This is indicated when the distance from the point, $\vec{P}^n$, and the starting point, $\vec{P}^1$, is less than a prescribed tolerance. If the point, $\vec{P}^n$, lies within the circle encompassing the starting point, $\vec{P}^1$, the mapping process is terminated.

Figure 12 is a generalized flow chart of the boundary mapping subroutine, RBNDRY. The intimate details of the logic are excluded.

III. PROGRAM OUTPUTS

In the example presented, the following base point data were used and are representative of a typical twin-jet fighter aircraft [7].

$$C_{Y_\beta} = -0.5730 \;,\; C_{Y_p} = 0.2460 \;,\; C_{Y_r} = 1.1060 \;,$$

$$C_{\ell_\beta} = -0.1570 \;,\; C_{\ell_p} = -0.2170 \;,\; C_{\ell_r} = 0.3050 \;,$$

$$C_{n_\beta} = 0.0808 \;,\; C_{n_p} = 0.0 \;,\; C_{n_r} = -0.606 \;.$$

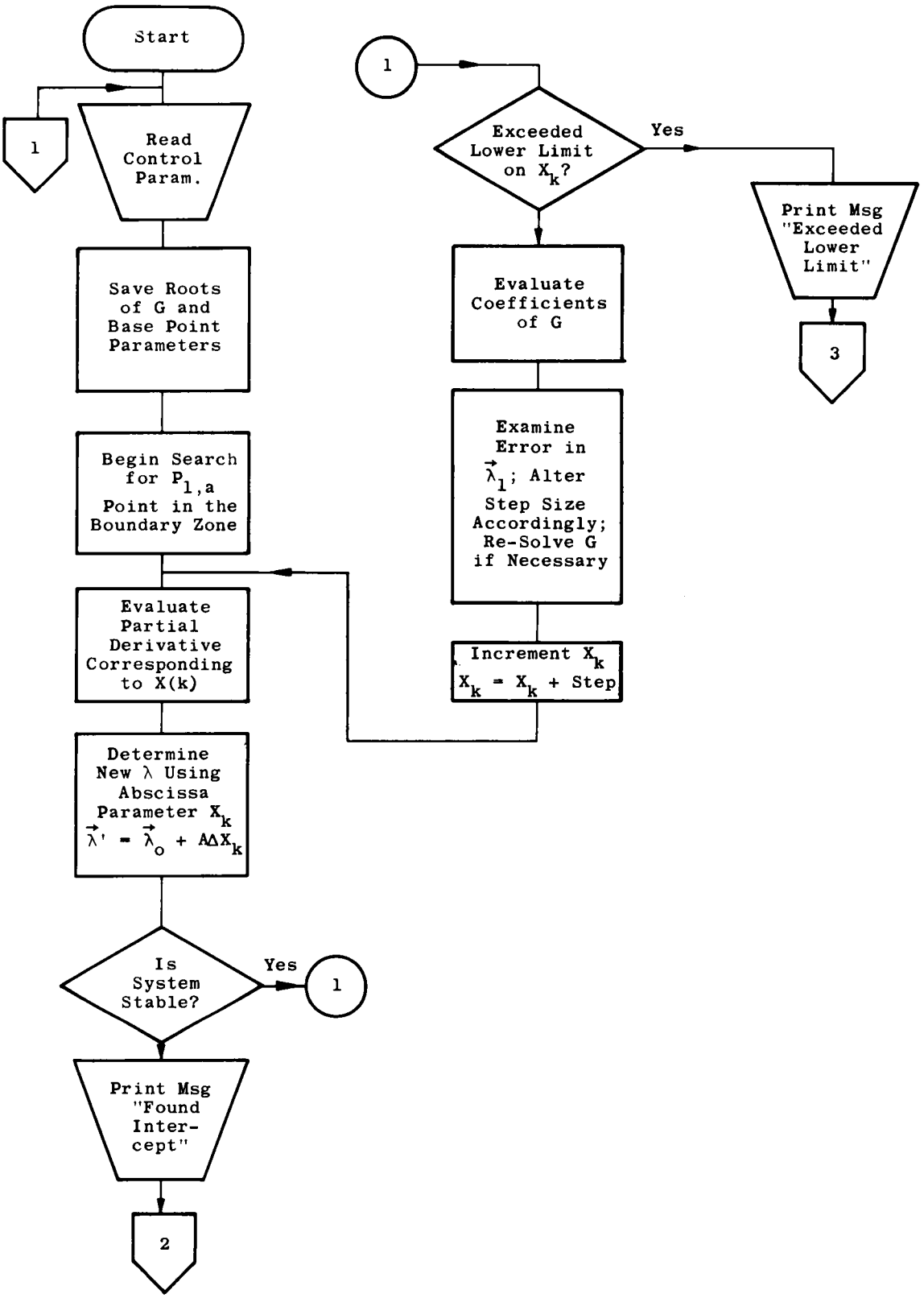


Figure 12. Flow diagram of boundary mapping routine.

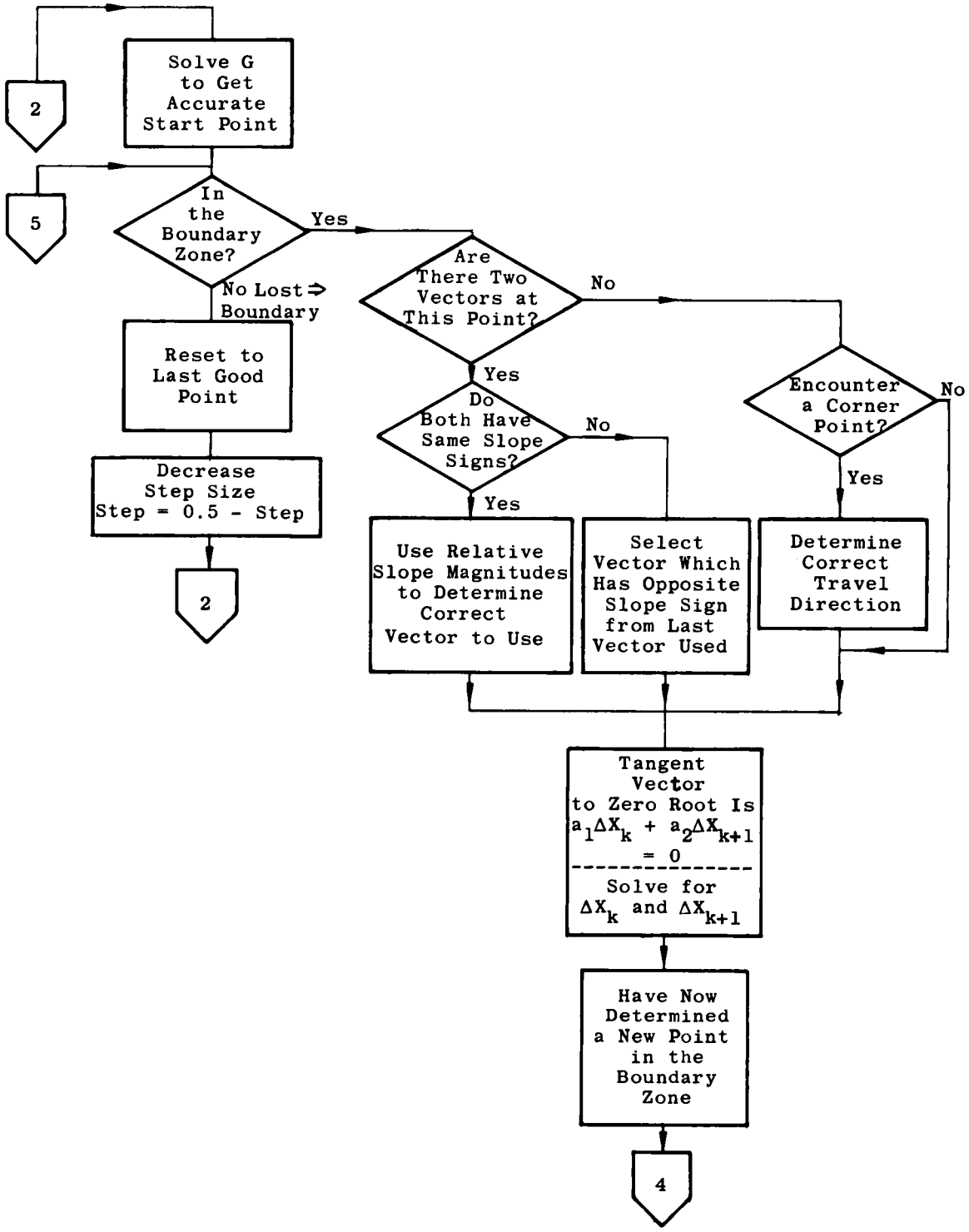


Figure 12. (continued)

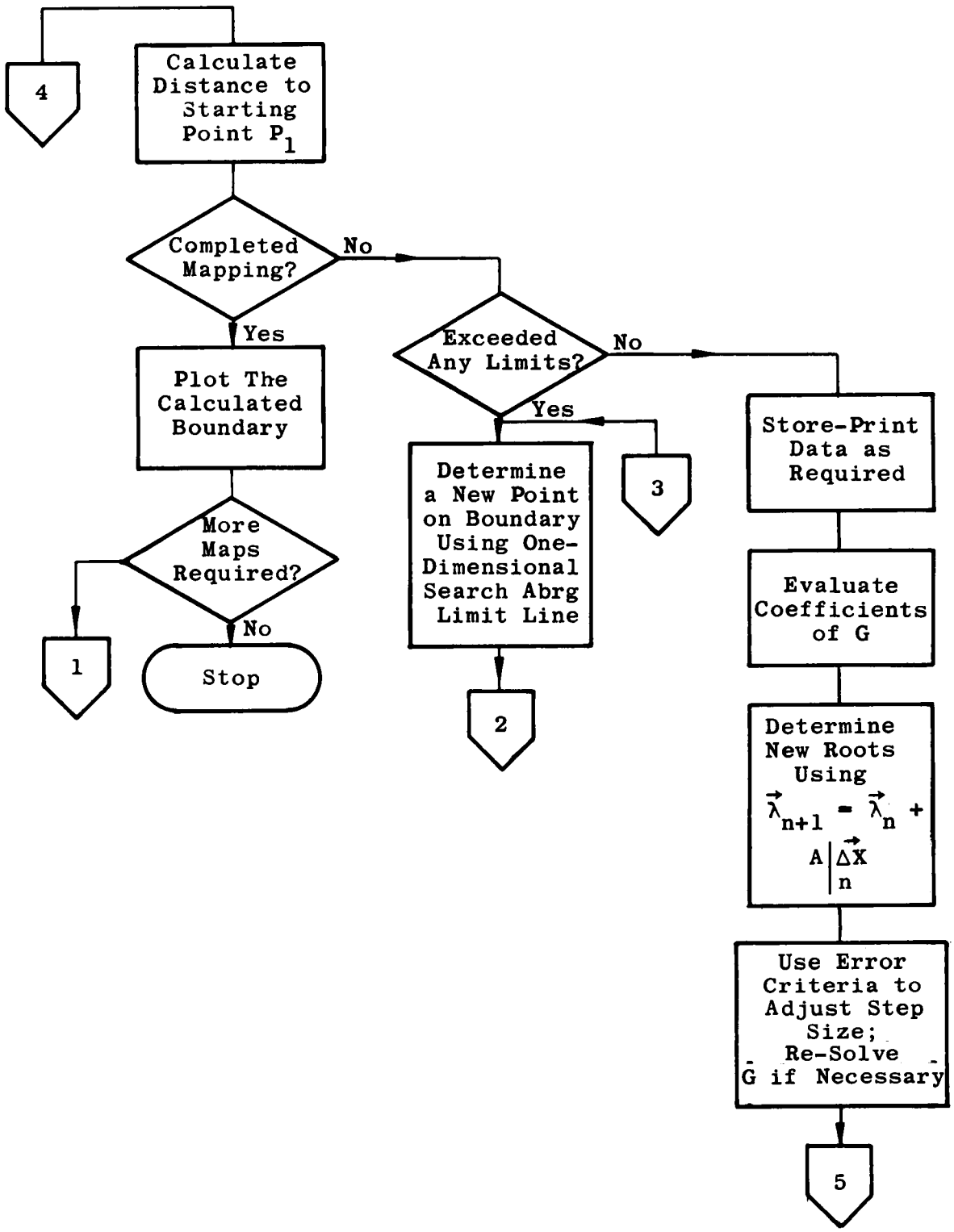


Figure 12. (continued)

The additional aircraft and flight condition data used are:

$$m = 1215.0 \ , \quad B = 38.41 \ , \quad S = 538.34 \ ,$$

$$I_x = 29{,}950 \ , \ I_z = 169{,}538 \ , \ I_{xz} = 5{,}241 \ ,$$

$$\text{Sigma} = 0.4485 \ , \quad Q = 87.8 \ , \quad V = 406.0 \ ,$$

$$\alpha = 15^\circ \ , \quad \theta = 15^\circ \ .$$

At the base point, the roots of the characteristic equation are:

$$\lambda_1 = -0.106 \ , \ \lambda_2 = -0.496 \ ,$$

$$\lambda_3 = -0.18 + 1.71j \ , \ \lambda_4 = -0.18 - 1.71j \ ,$$

and are referred to in the following discussion as the poles. The roots correspond to the spiral mode, the rolling mode, and the Dutch roll motion. The root locus plots shown in Figure 13 illustrate the effects that variations in several stability derivatives have on the lateral stability characteristics. The zero equations corresponding to each of the aerodynamic parameters are determined using Equation (III-1) and are summarized in Appendix II.

Figure 14 illustrates a stability region map obtained using the computer program for the aerodynamic parameters, C_{n_β} and C_{ℓ_β}. The base point is denoted $\vec{P}^0$ and the first point obtained on the boundary is denoted $\vec{P}^1$. The

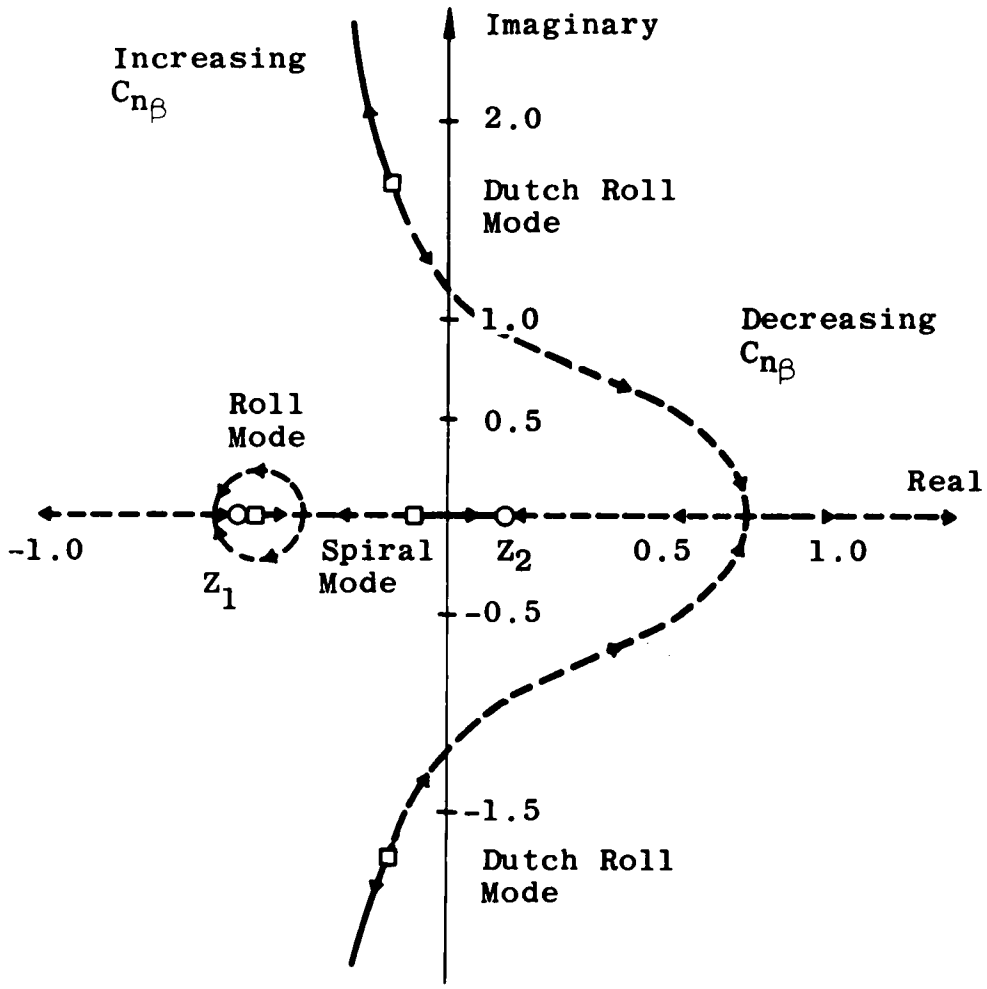


Figure 13. Sample root locus plot obtained using the lateral stability computer program.

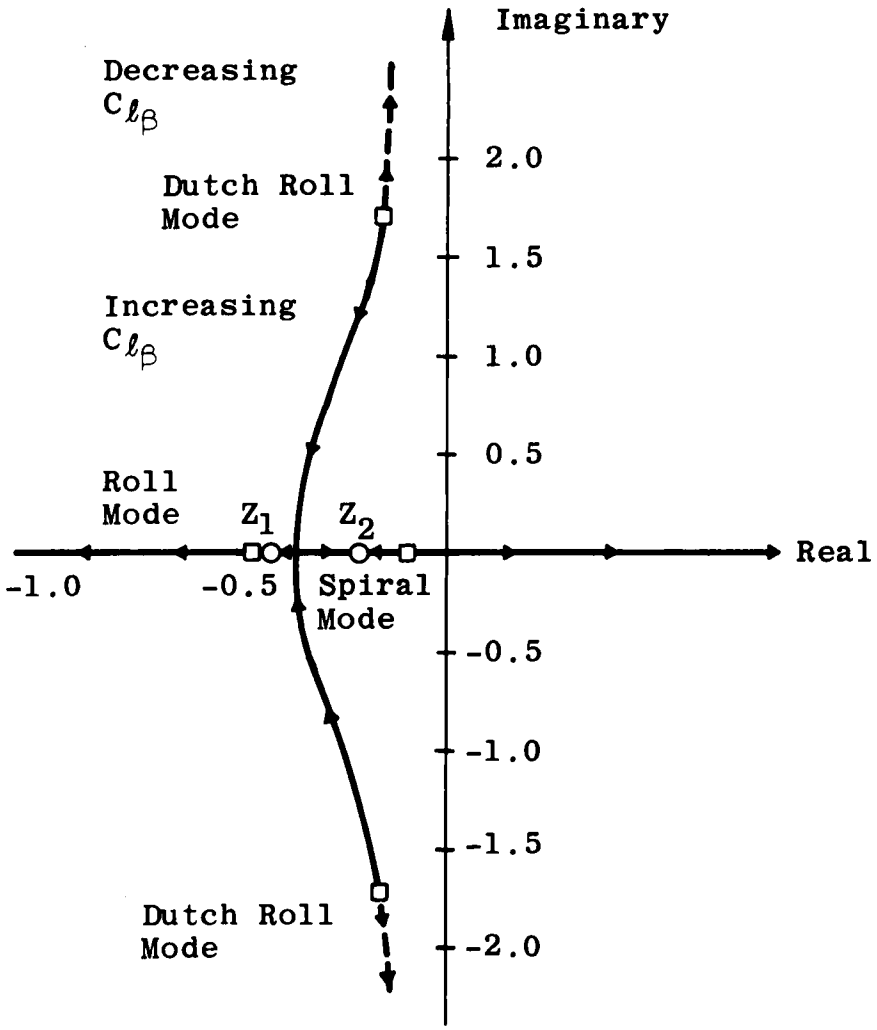


Figure 13. (continued)

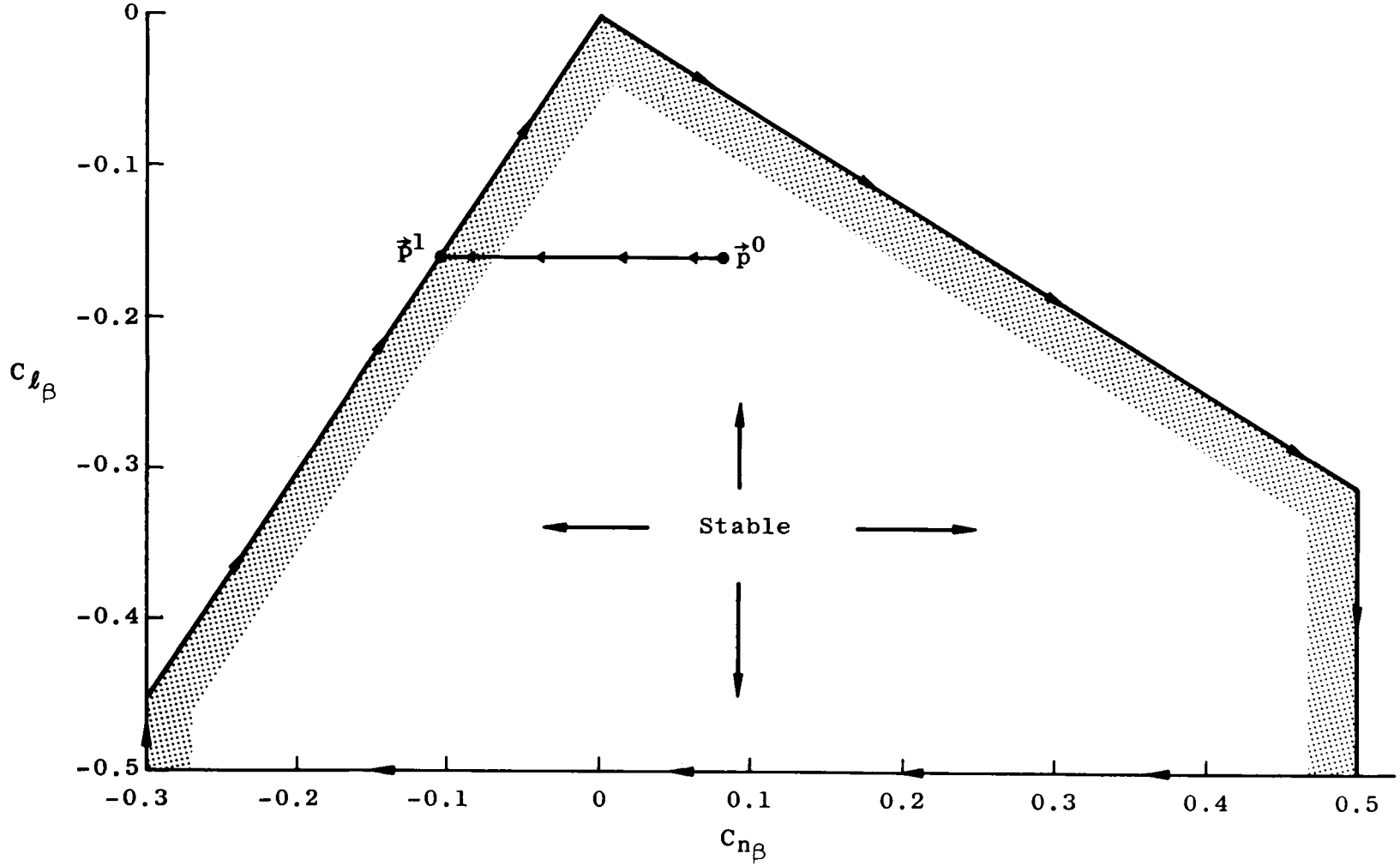


Figure 14. Sample stability region map obtained using the lateral stability computer program.

linear character of the boundary is a result of the coefficient functions of the characteristic equation being linear in C_{n_β} and C_{ℓ_β}. The origin represents a multiple root point.

Figure 15 illustrates constant λ lines which have been constructed throughout the stability region. The λ lines correspond to the spiral and rolling mode roots, λ_1 and λ_2. It can be seen then that the right part of the boundary represents the part of the region where the spiral mode becomes unstable. The line of $\lambda = 0.37$ represents a line of multiple roots. All along this line, the spiral and rolling mode roots are equal and become complex in the area shaded.

Figure 16 illustrates constant frequency and damping lines for the Dutch roll roots. It can be seen that the left part of the boundary represents the points in the $C_{n_\beta}, C_{\ell_\beta}$ plane where the Dutch roll roots become unstable.

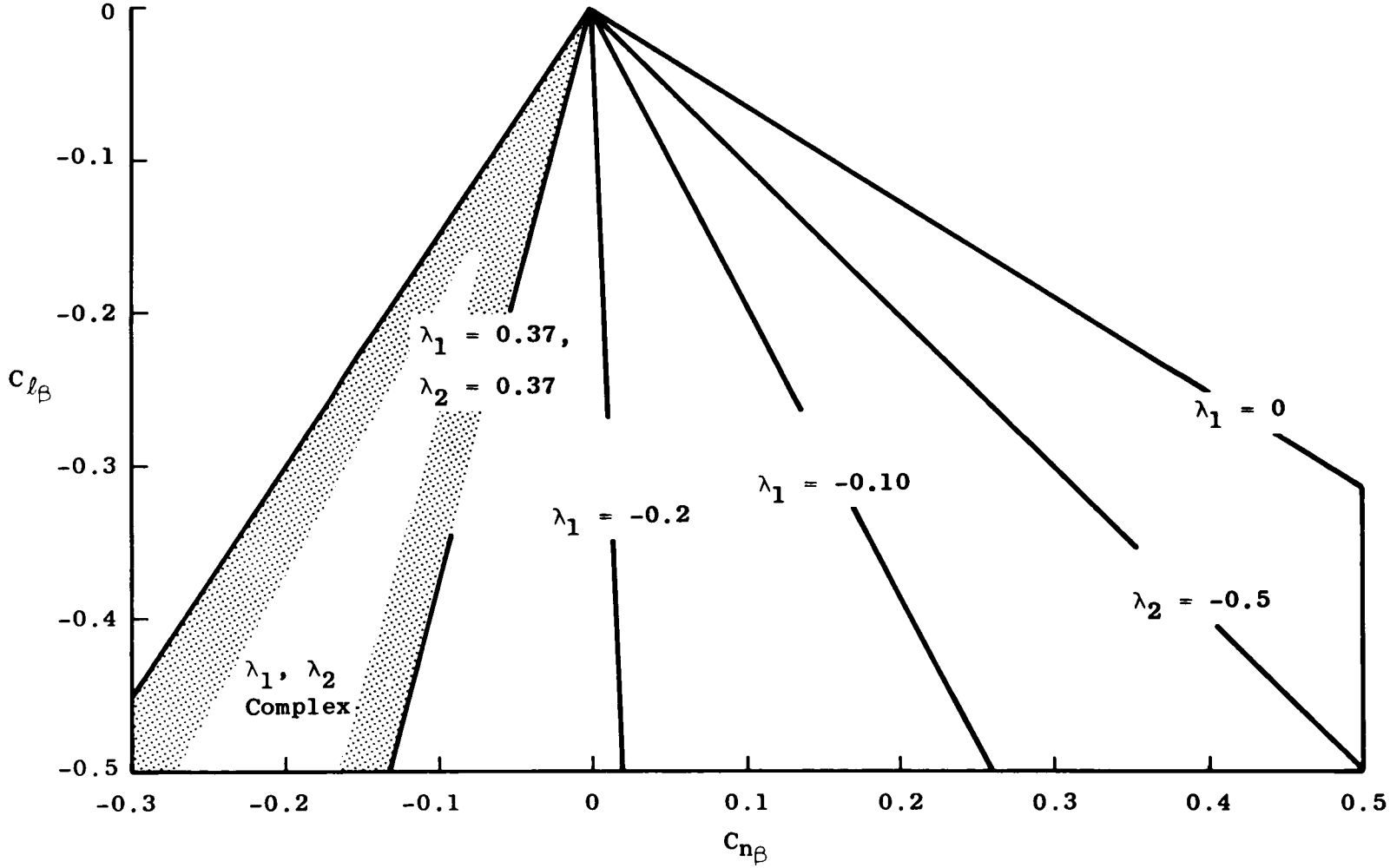


Figure 15. Detailed stability map illustrating the spiral and roll roots.

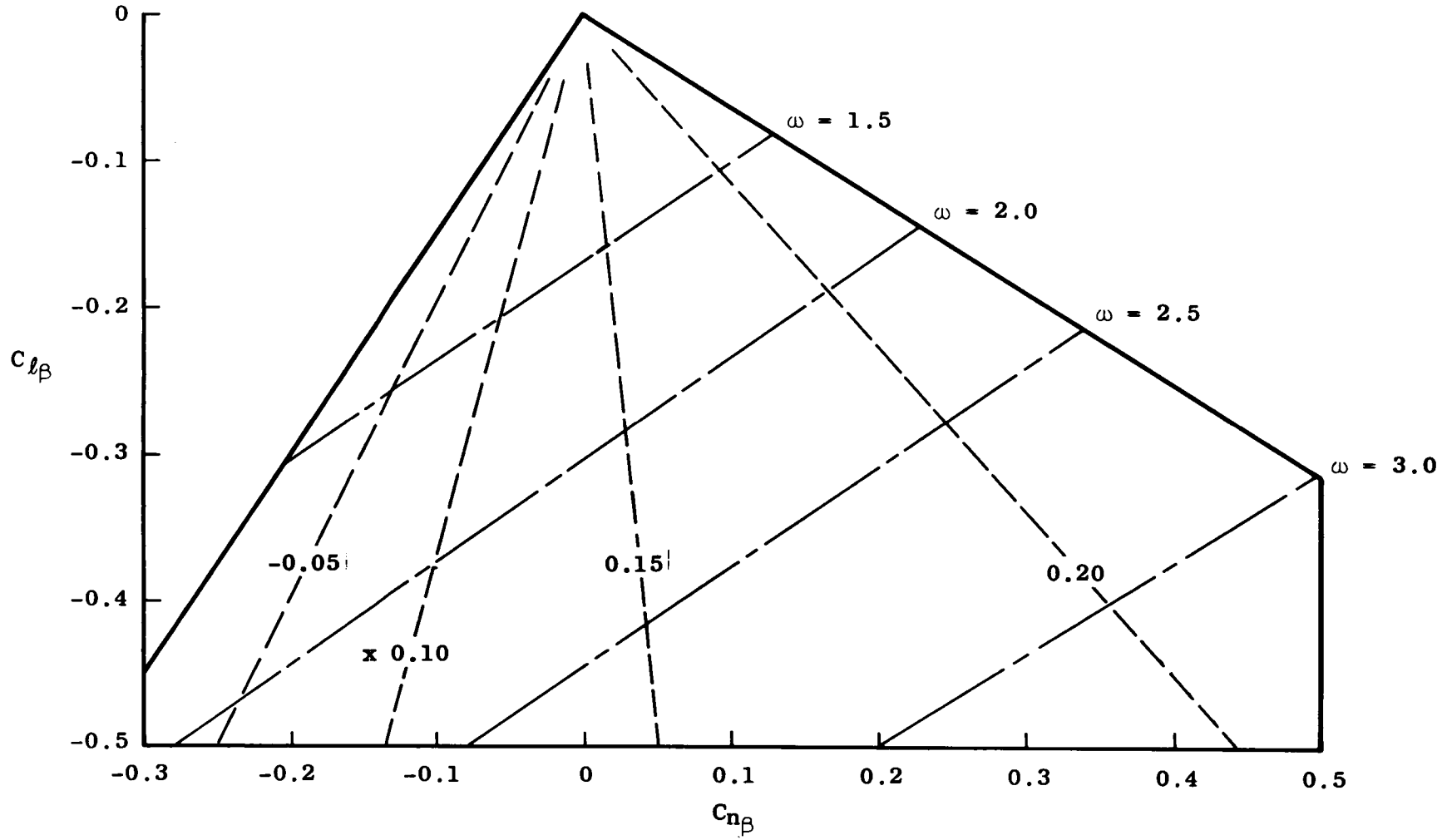


Figure 16. Detailed stability map illustrating the Dutch roll roots.

BIBLIOGRAPHY

BIBLIOGRAPHY

1. Kaplan, W. Ordinary Differential Equations. Reading, Massachusetts: Addison-Wesley Publishing Company, 1967.

2. Kaplan, W. Advanced Calculus. Reading, Massachusetts: Addison-Wesley Publishing Company, 1959.

3. Rosenbach, J. B., E. A. Whitman, B. E. Meserve, and P. M. Whitman. College Algebra. Fourth edition. Boston: Ginn and Company, 1958.

4. Etkin, B. Dynamics of Flight. New York: John Wiley and Sons, Inc., 1959.

5. Stapleford, R. L., D. E. Johnston, G. L. Teper, and D. H. Weir. "Development of Satisfactory Lateral-Directional Handling Qualities in the Landing Approach," National Aeronautics and Space Administration CR-239, Washington, D. C., July, 1965.

6. Thelander, J. A. "Aircraft Motion Analysis," Technical Documentary Report No. FDL-TDR-64-70, Wright-Patterson Air Force Base, Ohio, March, 1965.

7. Chambers, J. R., and E. L. Anglin. "Analysis of Lateral-Directional Stability Characteristics of a Twin-Jet Fighter Airplane at High Angles of Attack," National Aeronautics and Space Administration TN-D-5361, Langley Research Center, Langley Station, Hampton, Virginia, August, 1969.

APPENDICES

APPENDIX I

LIST OF SYMBOLS

$\vec{X}$	Design parameter column vector, $\vec{X} = (x_1, x_2, \cdots, x_\ell)$
$\Delta\vec{X}$	Incremental design parameter column vector
$F_i(\vec{X})$	Characteristic equation coefficient function
$\vec{\lambda}$	Eigenvalue column vector, $\vec{\lambda} = (\lambda_1, \lambda_2, \cdots, \lambda_n)$
$\Delta\vec{\lambda}$	Incremental eigenvalue column vector
$\vec{P}^m$	Design parameter values at the mth point, $\vec{P}^m = (x_1^m, x_2^m, \cdots, x_\ell^m)$
$\vec{P}_k^m$	Design parameter values at the mth point and the value of the kth eigenvalue at that point
$\vec{\lambda}^k$	Eigenvalues at the kth point, $\vec{\lambda}^k = (\lambda_1^k, \lambda_2^k, \cdots, \lambda_n^k)$
P_i	The ith pole represents a point in the complex plane given by the value of the ith eigenvalue at the base point
Z_i	The ith zero point
ω	Radian frequency
b	Wing span, ft
C_ℓ	Rolling moment coefficient, $M_x/q_\infty sb$
C_n	Yawing moment coefficient, $M_z/q_\infty sb$
C_Y	Side force coefficient, $F_Y/q_\infty s$
F_Y	Side force, lb
I_x	Moment of inertia about longitudinal body axis, slug-ft^2

I_z	Moment of inertia about normal body axis, slug-ft^2
m	Airplane mass, slugs
M_x	Rolling moment, ft-lb
M_z	Yawing moment, ft-lb
p	Rolling velocity, rad/sec
q_∞	Free-stream dynamic pressure, lb/ft^2
r	Yawing velocity, rad/sec
S	Wing area, ft^2
V	Velocity, ft/sec
β	Angle of sideslip, deg or rad
ρ	Mass density of air, slugs/ft^3
α	Angle of attack, deg or rad
θ	Angle of pitch, deg or rad
C_1	$\dfrac{1}{\left(1 - \dfrac{I_{xz}^2}{I_x I_z}\right)}$
C_2	$\dfrac{I_{xz}}{I_x}$
C_3	$\dfrac{I_{xz}}{I_z}$
L_r	$\dfrac{\rho S b^2 V}{4 I_x} C_{\ell_r}$
L_p	$\dfrac{\rho S b^2 V}{4 I_x} C_{\ell_p}$
L_v	$\dfrac{\rho S b V^2}{I_x} C_{\ell_\beta}$

$N_r \qquad \frac{\rho S b^2 V}{4 I_z} C_{n_r}$

$N_p \qquad \frac{\rho S b^2 V}{4 I_z} C_{n_p}$

$N_v \qquad \frac{\rho S b V^2}{I_z} C_{n_\beta}$

$Y_r \qquad \frac{\rho S b}{4m} C_{Y_r}$

$Y_p \qquad \frac{\rho S b}{4m} C_{Y_p}$

$Y_v \qquad \frac{\rho S V}{2m} C_{Y_\beta}$

$C_{\ell_\beta} \qquad \frac{\partial C_\ell}{\partial \beta}$

$C_{\ell_p} \qquad \frac{\partial C_\ell}{\partial \frac{pb}{2V}}$

$C_{\ell_r} \qquad \frac{\partial C_\ell}{\partial \frac{rb}{2V}}$

$C_{n_\beta} \qquad \frac{\partial C_n}{\partial \beta}$

$C_{n_p} \qquad \frac{\partial C_n}{\partial \frac{pb}{2V}}$

$$C_{n_r} \qquad \frac{\partial C_n}{\partial \frac{rb}{2V}}$$

$$C_{Y_\beta} \qquad \frac{\partial C_Y}{\partial \beta}$$

$$C_{Y_p} \qquad \frac{\partial C_Y}{\partial \frac{pb}{2V}}$$

$$C_{Y_r} \qquad \frac{\partial C_Y}{\partial \frac{rb}{2V}}$$

APPENDIX II

LATERAL STABILITY CHARACTERISTIC EQUATION

$$G = \lambda^4+F_3(\vec{X})\lambda^3+F_2(\vec{X})\lambda^2+F_1(\vec{X})\lambda+F_0(\vec{X})$$

where

$$F_3(\vec{X}) = -Y_v-C_1(L_p+C_2N_p+N_r+C_3L_r)$$

$$\begin{aligned}F_2(\vec{X}) = {} & C_1[Y_v(N_r+C_3L_r+L_p+C_2N_p)+(N_v+C_3L_v)(\cos\alpha-Y_r) \\ & -(L_v+C_2N_v)(\sin\alpha+Y_p)+(N_r+C_3L_r)(L_p+C_2N_p) \\ & -(N_p+C_3L_p)(L_r+C_2N_r)]\end{aligned}$$

$$\begin{aligned}F_1(\vec{X}) = {} & C_1\{Y_v[(N_p+C_3L_p)(L_r+C_2N_r)-(N_r+C_3L_r)(L_p+C_2N_p)] \\ & +(N_v+C_3L_v)[C_1Y_r(L_p+C_2N_p)-C_1\cos\alpha(L_p+C_2N_p) \\ & -\tfrac{g}{v}\sin\theta-C_1Y_p(L_r+C_2N_r)-C_1\sin\alpha(L_r+C_2N_r)] \\ & +(L_v+C_2N_v)[-Y_rC_1(N_p+C_3L_p)+C_1\cos\alpha(N_p+C_3Y_r) \\ & -\tfrac{g}{v}\cos\theta+C_1Y_p(N_r+C_3L_r)+C_1\sin\alpha(N_r+C_3L_r)]\}\end{aligned}$$

$$\begin{aligned}F_0(\vec{X}) = {} & C_1\{\tfrac{g}{v}\cos\theta[N_r+C_3L_r)(L_v+C_2N_v)-(N_v-C_3L_v)(L_r+C_2N_r)] \\ & -\tfrac{g}{v}\sin\theta[(L_v+C_2N_v)(N_p+C_2L_p)-(L_p+C_3N_p)(N_v+C_3L_v)]\}\ .\end{aligned}$$

The design parameter zero equations are:

$$\partial G/\partial x_1 = -\lambda^3 + C_1[x_9 + C_3x_6 + x_5 + C_2x_8]\lambda^2 + C_1^2[(x_8 + C_3x_5)(x_6 + C_2x_9) - (x_9 + C_3x_6)(x_5 + C_2x_8)]\lambda$$

$$\partial G/\partial x_2 = -C_1[x_4 + C_2x_7]\lambda^2 + C_1^2[-(x_7 + C_3x_4)(x_6 + C_2x_9) + (x_4 + C_2x_7)(x_9 + C_3x_6)]\lambda$$

$$\partial G/\partial x_3 = -C_1[x_7 + C_3x_4]\lambda^2 + C_1^2[(x_7 + C_3x_4)(x_5 + C_2x_8) - (x_4 + C_2x_7)(x_8 + C_3x_5)]\lambda$$

$$\partial G/\partial x_4 = C_1[C_3(\cos\alpha - x_3) + (-\sin\alpha - x_2)]\lambda^2 + C_1[C_3\{C_1x_3(x_5 + C_2x_8) - C_1\cos\alpha(x_5 + C_2x_8) - \frac{g}{v}\sin\theta - C_1(x_6 + C_2x_9)x_2 - C_1(x_6 + C_2x_9)\sin\alpha\} + \{-C_1x_3(x_8 + C_3x_5) + C_1\cos\alpha(x_8 + C_3x_5) - \frac{g}{v}\cos\theta + C_1x_2(x_9 + C_3x_6) + C_1\sin\alpha(x_9 + C_3x_6)\}]\lambda + C_{1v}^{2g}[\cos\theta(1 - C_2C_3)x_9 - \sin\theta\{(x_8 + C_2x_5) - C_3(x_5 + C_3x_8)\}]$$

$$\partial G/\partial x_5 = -C_1\lambda^3 + C_1[x_1 + C_1x_9(1-C_2C_3)]\lambda^2 + C_1^2[C_1C_3x_1(x_6+C_2x_9)$$

$$-x_1(x_9+C_3x_4) + (x_7+C_3x_4)(x_3-\cos\alpha) + (x_4+C_2x_7)$$

$$(-x_3+\cos\alpha)C_3]\lambda + C_1^2[-\frac{g}{v}\sin\theta\{C_2(x_4+C_2x_7) - (x_7+C_3x_4)\}]$$

$$\partial G/\partial x_6 = -C_1C_3\lambda^3 + C_1[C_3\{x_1 + C_1(x_5+C_2x_8)\} - C_1(x_8+C_3x_5)]\lambda^2$$

$$+C_1^2[x_1(x_8+C_3x_5) + (x_7+C_3x_4)(-x_2-\sin\alpha)$$

$$+(x_4+C_2x_7)(C_3x_2+C_3\sin\alpha)]\lambda$$

$$+C_1^2[\frac{g}{v}\cos\theta x_7(C_2C_3-1)]$$

$$\partial G/\partial x_7 = C_1[\cos\alpha - x_3 - C_2\sin\alpha - C_2x_2]\lambda^2 + C_1[\{x_3C_1(x_5+C_2x_8)$$

$$-C_1\cos\alpha(x_5+C_2x_8) - \frac{g}{v}\sin\theta - C_1(x_6+C_2x_9)x_2$$

$$-C_1(x_6+C_2x_9)\sin\alpha\} + C_2\{-C_1x_3(x_8+C_3x_5) + C_1\cos\alpha(x_8+C_3x_5)$$

$$-\frac{g}{v}\cos\theta + C_1(x_9+C_3x_6)x_2 + C_1(x_9+C_3x_6)\sin\alpha\}]\lambda$$

$$+C_1^2\frac{g}{v}[\cos\theta(C_2C_3-1)x_6 - \sin\theta\{C_2(x_8+C_2x_5) - (x_5+C_3x_8)\}]$$

$$\partial G/\partial x_8 = -C_1C_2\lambda^3 + [C_1C_2x_1 + C_1C_2(C_1x_9 + C_1C_3x_6) - C_1(C_1x_6 + C_1C_2x_9)]\lambda^2$$

$$+ [x_1\{C_1(C_1x_6 + C_1C_2x_9) - C_1C_2(C_1x_9 + C_1C_3x_4)\}$$

$$+ (C_1x_7 + C_1C_3x_4)(C_1C_2x_3 - C_1C_2\cos\alpha) + (C_1x_4 + C_1C_2x_7)$$

$$(-C_1x_3 + C_1\cos\alpha)]\lambda + [-\frac{g}{v}\sin\theta\{C_1(C_1x_4 + C_1C_2x_7)$$

$$-C_1C_3(C_1x_7 + C_1C_3x_4)\}]$$

$$\partial G/\partial x_9 = -C_1\lambda^3 + [C_1x_1 + C_1(C_1x_5 + C_1C_2x_8) - C_1C_2(C_1x_8 + C_1C_3x_5)]\lambda^2$$

$$+ [C_1C_2x_1(C_1x_8 + C_1C_3x_5) - C_1x_1(C_1x_5 + C_1C_2x_8)$$

$$+ (C_1x_7 + C_1C_3x_4)(-C_1C_2x_2 - C_1C_2\sin\alpha) + (C_1x_4 + C_1C_2x_7)$$

$$(C_1x_2 + C_1\sin\alpha)]\lambda + [\frac{g}{v}\cos\theta\{C_1(C_1x_4 + C_1C_2x_7)$$

$$-C_1C_2(C_1x_7 + C_1C_3x_4)\}] .$$

VITA

James L. Taylor was born in Chattanooga, Tennessee, on November 3, 1942. He attended elementary schools in that city and was graduated from Central High School in 1959. The following November he joined the United States Navy and served as an electronics technician. He was honorably discharged from the United States Navy in November, 1963.

In February, 1964, he accepted employment with ARO, Inc., as an instrument technician. In June, 1967, he entered Middle Tennessee State University, and in August, 1970, received a Bachelor of Science degree with a major in Mathematics. In November, 1970, he accepted a position as a mathematician with the United States Naval Weapons Laboratory in Dahlgren, Virginia. He has been employed by ARO, Inc., since February, 1972, as an instrument engineer.

He entered the Graduate School at The University of Tennessee Space Institute in June, 1972, and received the Master of Science degree with a major in Mathematics in December, 1974.

He is married to the former Wilma Yvonne Prater of McMinnville, Tennessee.